Accepted Manuscript

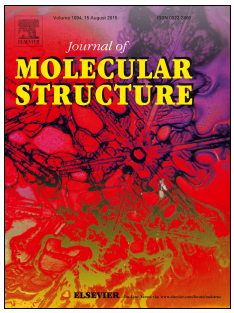

Spectroscopic studies of aryl substituted 1-phenyl-2-pyrazolines: Steric and electronic substitution effects

Marzieh Soltani, Hamid R. Memarian, Hassan Sabzyan

PII: S0022-2860(18)30871-8

DOI: 10.1016/j.molstruc.2018.07.052

Reference: MOLSTR 25457

To appear in: *Journal of Molecular Structure*

Received Date: 28 May 2018

Revised Date: 14 July 2018

Accepted Date: 16 July 2018

Please cite this article as: M. Soltani, H.R. Memarian, H. Sabzyan, Spectroscopic studies of aryl substituted 1-phenyl-2-pyrazolines: Steric and electronic substitution effects, *Journal of Molecular Structure* (2018), doi: 10.1016/j.molstruc.2018.07.052.

Graphical Abstract

σ- or π-donor/acceptor ability effects of the C_3- and C_5-aryl substitutions on the UV-Vis, IR and NMR spectral data in 2-pyrazolines were investigated experimentally and theoretically. Marzieh Soltani, Hamid R. Memarian and Hassan Sabzyan.

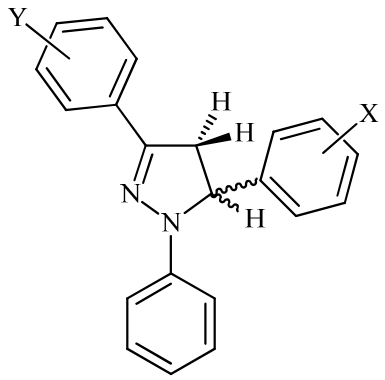

Spectroscopic studies of aryl substituted 1-phenyl-2-pyrazolines: steric and electronic substitution effects

Marzieh Soltani, Hamid R. Memarian* and Hassan Sabzyan*

Department of Chemistry, University of Isfahan, 81746-73441 Isfahan, I. R. Iran.

Abstract. A series of aryl substituted 1-phenyl-2-pyrazolines containing electron-donating and electron-withdrawing substituents on different positions of the C_3- or C_5-aryl groups were synthesized and their steric and electronic effects on characteristic spectral data were investigated by experimental spectroscopic methods (UV-Vis, IR and NMR) and DFT computations. Whereas the C_5-aryl group of the heterocyclic ring behaves as σ-donor/acceptor substituent, the π-donor/acceptor ability of the C_3-aryl group depends on the co-planarity of the substituent with the aryl ring and also the extent of the orientation of this C_3-aryl ring towards the C=N double bond of the heterocyclic ring. A significant through conjugation of the lone pair on the N_1-atom towards the C_3-aryl ring is observed when the electron-withdrawing nitro group is located on the *para*-position of this aryl ring. The experimental spectroscopic results for the substitution effects are also supported by (TD)DFT/6-311++G(d,p) computed UV-Vis spectra. Experimental and theoretical NMR chemical shifts and spin-spin coupling constants obtained for these 2-pyrazolines validated by Karplus diagram approves the structures predicted for these compounds.

Keywords. UV-Vis, IR and NMR Spectroscopies; Electronic and steric effects; 2-Pyrazolines; TD-DFT.

1. Introduction

The study and synthesis of nitrogen containing heterocyclic compounds are significant due to the fact that these compounds have various pharmaceutical and medical properties. 2-

Pyrazolines or 4,5-dihydropyrazoles and their oxidized form, pyrazoles (Scheme 1) are one of the important class of heterocyclic compounds containing two adjacent nitrogen atoms, which have different biological activities [1-8].

Scheme 1

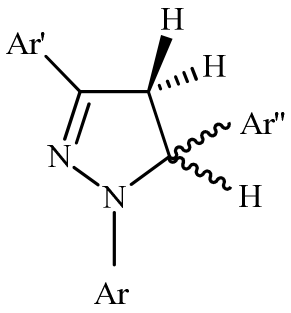

4,5-Dihydropyrazoles

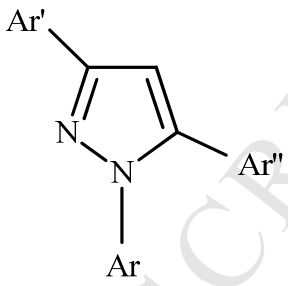

Pyrazoles

Various works are devoted to elucidate the electronic effects of the heterocyclic ring substitutions in 2-pyrazolines on some characteristic features of these compounds. The electronic effects of ring substitutions in some 1-acetylpyrazolines and 2-naphthylpyrazolines on the chemical shifts of characteristic heterocyclic ring hydrogens were investigated by correlation of their spectral properties with the Hammett substituent constant and the Swain-Lupton parameters [9,10]. In other studies, electronic effects of ring substitutions on the photophysical properties, X-ray analysis and DFT B3LYP computational results were also reported [11-13].

Our research interest concerns investigation of the steric and electronic factors of substituents affecting the rate of thermal and photochemical oxidation, and cyclic voltammetric measurement of nitrogen-containing heterocyclic compounds such as 1,4-dihydropyridines [14], 2-oxo-1,2,3,4-tetrahydropyrimidines [15-18], and 2,3-dihydroquinazolinones [19,20] and 2-oxo-1,2,3,4-tetrahydropyridines [21,22].

In continuation to our previous studies, we decided to synthesis various 3- or 5-aryl substituted 1-phenyl-2-pyrazolines containing electron-donor and electron-acceptor

substituents on 3- or 5-aryl positions, in order to elucidate their steric and electronic (inductive and resonance) effects on the UV-Vis, ^{1}H NMR and IR spectra and also on the DFT computational results.

2. Experimental and Computational Methods

2.1. Material and Synthetic Methods. All chemical used were purchased from Alfa Aesar, Merck and Sigma-Aldrich companies. Melting points have been determined in open glass capillaries on a Stuart Scientific SMP2 apparatus and are not corrected. Infrared spectra have been recorded from KBr-discs on a Jasco FT/IR-6300 spectrometer. The ^{1}H NMR and ^{13}C NMR spectra (DMSO-d_6 or $CDCl_3$) have been recorded on Bruker Avance III 400 spectrometers at 400 and 100 MHz at room temperature. The ^{1}H NMR spectra are reported as follows: chemical shifts, [multiplicity, number of protons, coupling constants *J* (Hz), and assignment]. UV spectra were taken with Cary (500 scan) spectrometer.

A mixture of substituted chalcones (1 mmol) and phenylhydrazine hydrochloride (2 mmol) in EtOH (7 mL) was heated at 100 ºC for appropriate time. After completion of the reaction indicated by TLC (*n*-hexane/ethyl acetate, 10:1), the reaction mixture was cooled to room temperature. The solid products were filtered and washed with cold ethanol. The pure products were obtained by recrystallization from ethanol. Physical and spectroscopic data are given in Appendix and the complete spectra are provided in Supporting Information.

2.2. Computational Method. Geometries of 2-pyrazolines (**1a-s**) are optimized using the density functional theory (DFT) B3LYP method with 6-311++G(d,p) basis set. The ^{1}H NMR chemical shifts of these optimized structures referenced to TMS were computed using the gauge-invariant atomic orbitals (GIAO) method at the same level of theory in the conductor-like polarizable continuum model (CPCM) solvent of DMSO. The nuclear-independent chemical shift (NICS) [23,24] is also calculated for a selected set of derivatives using independent individual gauges for atoms in molecules method (IGAIM). Time-dependent

density functional theory (TD-DFT) B3LYP/6-311++G(d,p) method considering 10 excited states is used in the presence of chloroform CPCM solvent. Furthermore, vibrational spectra are calculated using harmonic oscillator analysis with a scale factor of 0.9614 [25]. All computations are carried out using G09 program [26].

3. Results and Discussion

In order to elucidate the steric and electronic effects of the aryl substitutions on the C_3- or C_5-positions of the heterocyclic ring on the spectroscopic behavior of the series of compounds considered in the present work, the synthesis of 2-pyrazolines was carried out by condensation of suitable chalcone precursors with phenylhydrazine hydrochloride in ethanol under reflux condition (Scheme 2). The specific data are summarized in Table 1.

Scheme 2

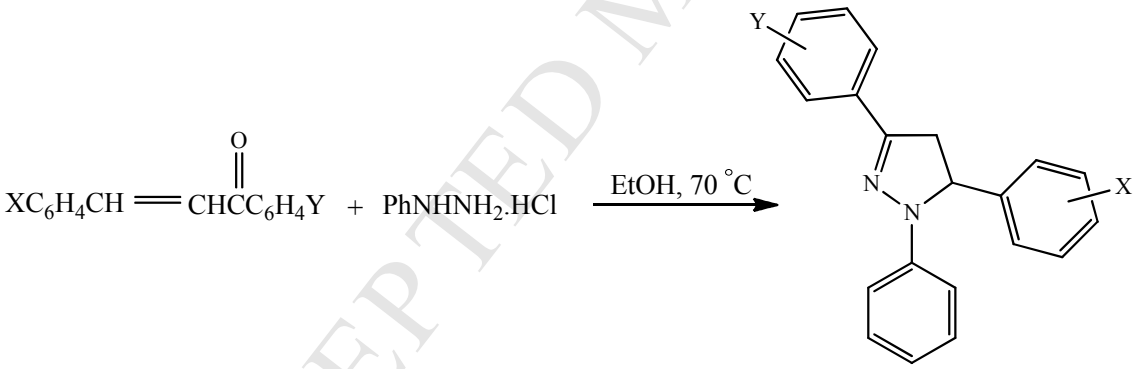

Table 1. Synthesized aryl substituted 2-pyrazoline compounds

Compound	Y	X	Time (h)	Yield (%)	M.P. (˚C)
1a	H	H	6	71	134-136
1b	4-Cl	H	8	82	148-150
1c	3-Cl	H	3	70	129-131
1d	2-Cl	H	5	45	122-125
1e	H	4-Cl	7	85	131-133
1f	H	3-Cl	3	87	106-108

1g	H	2-Cl	2.75	60	134-136
1h	4-MeO	H	2	70	141-143
1i	3-MeO	H	4	45	126-128
1j	2-MeO	H	6	90	160-162
1k	H	4-MeO	7	50	123-125
1l	H	3-MeO	6.5	90	92-95
1m	H	2-MeO	7.5	64	130-132
1n	4-NO_2	H	2	76	180-183
1o	3-NO_2	H	7	60	134-136
1p	2-NO_2	H	6	40	146-148
1q	H	4-NO_2	5.8	40	113-116
1r	H	3-NO_2	7	62	123-125
1s	H	2-NO_2	4	57	136-138

The synthesized compounds were identified by obtaining and analyzing their ^{1}H NMR, UV-Vis and IR spectra. The substituted aryl ring on the C_5-position of the heterocyclic ring behaves as either a σ-donor or a σ-acceptor group due to its attachment to the sp^3 hybridized carbon atom. While, the substituted aryl ring on the C_3-position of the heterocyclic ring can possibly act as either a π-donor or a π-acceptor substituent. The C_3-aryl ring is attached to the sp^2 hybridized carbon atom of the C=N double bond of the heterocyclic ring. Therefore, its orientation relative to this double bond and also the possible co-planarity of the additional substituent on the C_3-aryl ring with this ring are important factors determining the extent of its π-electron donor/acceptor ability.

The σ-donor/acceptor ability of substituted aryl ring on the C_5-position depends on the electronic nature and position of the additional substituent on this ring. For example, the methoxy group (CH_3O) on each position of the C_5-aryl ring (as in **1k**, **1l** and **1m**) acts as a σ-acceptor group because of the inductive effect of its oxygen atom, whereas possible co-planar orientation of this group especially on the *para*- and *ortho*-positions with the C_5-aryl ring (**1k**

and **1m**) results in the delocalization of its oxygen lone pair towards the C-aryl ring (C_{18}) attached to the C_5-atom of the heterocyclic ring. Consequently, as a balance of both negative inductive and positive resonance effects of the methoxy group, this group behaves as a σ-donor and thus an increase in the electron density of the heterocyclic ring *via* the σ-bond (C_5–C_{18}) is expected. In contrast to the behaviour of the methoxy group, the nitro group (NO_2) on the C_5-aryl ring behaves as a σ-acceptor substituent on each position of the aryl ring due to its electron-withdrawing character. In the case of co-planar orientation of this group with the aryl ring, especially on the *para*- and *ortho*-positions (**1q** and **1s**), delocalization of the π-electrons towards the NO_2 group *via* resonance causes a decrease of the electron density on the C_{18}-atom attached to the C_5-atom, making its electron-withdrawing character more pronounced. As a results of both negative inductive and negative resonance effects of the NO_2 group, a decrease of the electron density of the heterocyclic ring *via* the C_5– C_{18} σ-bond is expected.

The strength of the π-donor or π-acceptor character of the substituted aryl ring attached to the C_3-position of the heterocyclic ring depends on the extent of co-planarity orientation of the additional substituent on the C_3-aryl ring, especially on the *para*- and *ortho*-positions, and also on the orientations of the C_3-aryl ring towards the C_3=N_2 double bond. Keeping these arguments in mind and considering also the orientation of the C_5-aryl ring towards the heterocyclic ring atoms, especially the C_4-methylene hydrogens, the results of the experimental spectroscopic data with the help of the results of DFT computational studies will explain comparative spectroscopic characteristics of this series of compounds.

Another point to be considered in the present study is the effect of the nature of the medium on some characteristic parameters in 2-pyrazolines. The attachment of the N_1 atom with phenyl ring and the conjugated imine double bond in the parent compound **1a**, as representative, allows delocalization of the N_1 lone pair either to the conjugated imine group

forming the resonance structure **RS-I** or to the N_1-phenyl ring forming the resonance structure **RS-II** as shown in Scheme 3. Due to the polar nature of DMSO solvent, it is expected that upon delocalization of the N_1-lone pair, the involvement of the zwitterionic resonance structures **RS-I** and **RS-II** are more possible than unionized molecular structure. The preference involvement of one of these resonance structures or unionized molecule certainly depends on the nature of the additional substituent on the aryl ring, which has already been observed in some of 2-pyrazoline derivatives [11,12].

Scheme 3

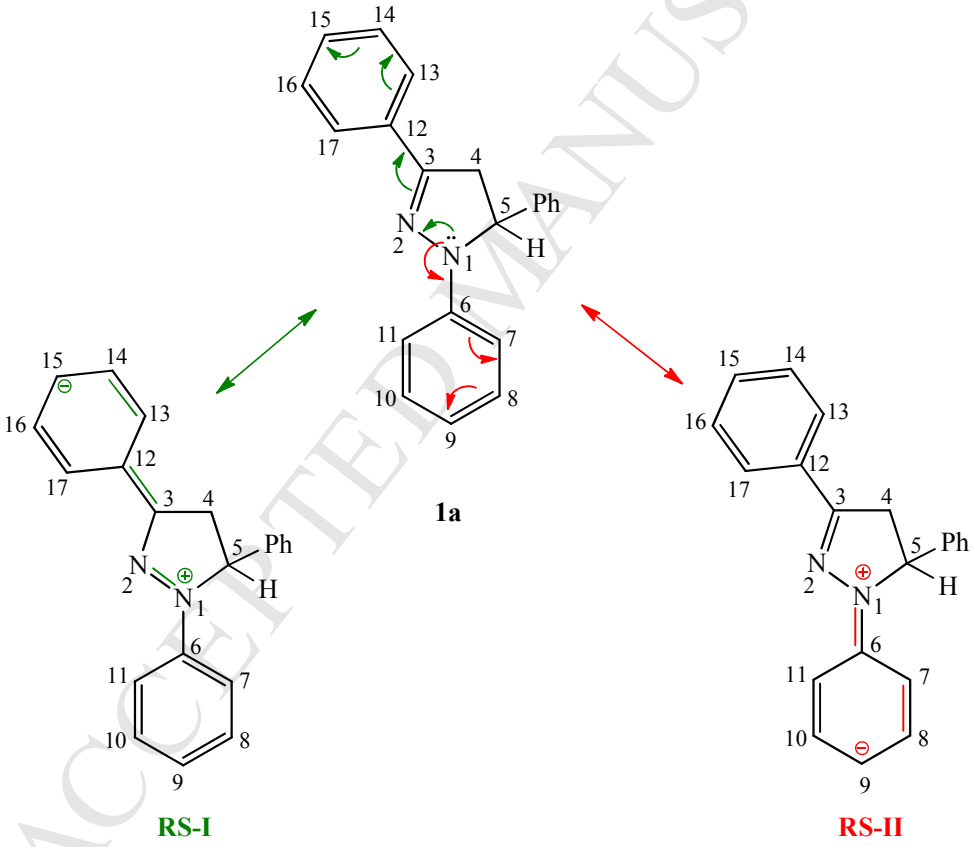

In order to elucidate the effect of solvent on the data obtained by computational and experimental studies, the optimized structures of 2-pyrazolines were obtained in the gas phase and also in DMSO solvent. Comparative analysis of the computational data of the parent compound **1a**, as an example, in both phases (Table 2, and the data of the remaining 2-

pyrazolines are provided in Table S1 of the Supporting Information) indicates that **1a** in DMSO medium seems to be more polar than in the gas phase, which is a result of more co-planar orientation of the N_1-phenyl ring towards the heterocyclic ring which allows better delocalization of the N_1-lone pair to this ring. Comparison of the bond lengths and dihedral angles given in Table 2 supports the preferred involvement of the resonance structure **RS-II** (Scheme 3). This contribution of the zwitterionic resonance structures is also supported by higher stabilization of the compound **1a** in DMSO (by ~25.54 kJ/mole) and the increased dipole moment (from 2.6 D to 4.0 D) in DMSO compared to that in the gas phase.

Table 2. The optimized values of selected bond lengths and angels obtained for the representative 2-pyrazoline **1a** in the gas phase and in the CPCM model of DMSO using B3LYP/6-311G++(d,p) method

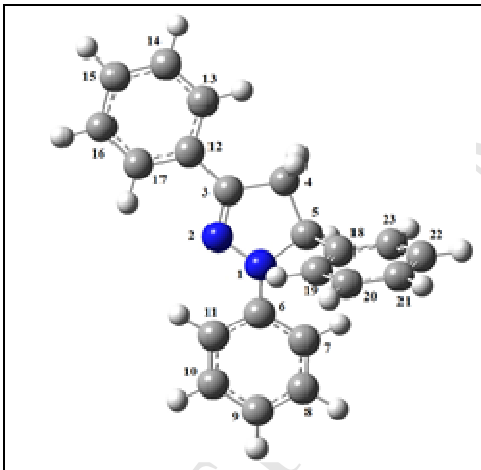

	Gas Phase	DMSO
N_1–N_2	1.3655	1.3672
N_1–C_6	1.3979	1.3918
N_1–C_5	1.4808	1.4827
N_2–C_3	1.2895	1.2909
C_3–C_{12}	1.4631	1.4643
C_5–H	1.0956	1.0933
α	-178.4	-176.7
β	-167.8	-172.9
γ	-94.6	-98.0
ω	0.7	3.8
α = N_2-C_3-C_{12}-C_{13}, β = C_5-N_1-C_6-C_{11} γ = C_4-C_5-C_{18}-C_{23}, ω = N_1-C_5-C_4-C_3		

3.1. NMR Studies

The condensation of the chalcon precursors and phenylhydrazine hydrochloride results in the formation of the enantiomeric pair for each 4,5-dihydropyrazole (**1a-s**) with the C_5-atom as the sole stereocenter. Analysis of the NMR spectra shows that, owing to the presence of this stereocenter, the hydrogens on the neighbouring C_4-atom are diastereotopic and appear as two doublet of doublets upon coupling with each other and further coupling with 5-H. Therefore, an AMX system, as expected, is observed for the geminal (4-CH_2) and vicinal (5-

CH) in the ^{1}H NMR spectra of **1a-s**. The benzylic proton H_x has the highest chemical shift among the three protons of the AMX system. Also, between the two H_A and H_M diastereotopic geminal protons, H_A is more shielded because of the *cis*-orientation with respect to the adjacent C_5-aryl ring which induces a ring current shielding effect on this proton. Characteristic ^{1}H chemical shifts and the corresponding coupling constants measured for 2,3-dihydropyrazoles (**1a-s**) are given in Table 3.

Table 3. Characteristic heterocyclic ring ^{1}H chemical shifts (δ, ppm) and coupling constants (J, Hz) of 2,3-dihydropyrazoles (**1a-s**) in DMSO-*d6* derived from their NMR spectra

1	Y	X	δ_A	J_{AM}	J_{AX}	δ_M	J_{AM}	J_{MX}	δ_X	J_{MX}	J_{AX}	δ_{MeO}
a	H	H	3.11	17.6	6.4	3.93	17.6	12.4	5.48	12.4	6.4	
b	4-Cl	H	3.11	17.2	6.4	3.91	17.6	12.4	5.51	12.4	6.4	
c	3-Cl	H	3.21	17.6	6.4	3.99	17.6	12.4	5.60	12.4	6.4	
d	2-Cl	H	3.22	17.4	6.2	4.05	17.4	12.2	5.50	12.2	6.2	
e	H	4-Cl	3.12	17.5	6.2	3.92	17.5	12.2	5.52	12.2	6.2	
f	H	3-Cl	3.16	17.6	6.4	3.92	17.6	12.0	5.53	12.4	6.4	
g	H	2-Cl	3.09	17.4	6.3	4.02	17.6	12.4	5.69	12.2	6.2	
h	4-MeO	H	3.08	17.4	6.6	3.80	17.4	12.2	5.42	12.2	6.6	3.79
i	3-MeO	H	3.11	17.6	6.4	3.91	17.6	12.4	5.48	12.4	6.4	3.81
j	2-MeO	H	3.17	18.0	6.4	3.98	18.0	12.0	5.39	12.0	6.4	3.77
k	H	4-MeO	3.08	17.6	6.4	3.88	17.6	12.0	5.43	12.0	5.8	3.71
l	H	3-MeO	3.11	17.4	6.4	3.91	17.4	12.2	5.44	12.2	6.4	3.71
m	H	2-MeO	3.01	17.4	6.0	3.92	17.4	12.1	5.62	12.1	6.0	3.92
n	4-NO_2	H	3.19	17.6	6.2	3.98	17.6	12.6	5.65	12.6	6.2	
o	3-NO_2	H	3.28	17.6	6.3	4.05	17.6	12.5	5.66	12.5	6.3	
p	2-NO_2	H	3.17	17.4	6.4	4.01	17.4	12.4	5.59	12.4	6.4	
q	H	4-NO_2	3.17	17.6	6.3	3.98	17.6	12.4	5.68	12.4	6.3	
r	H	3-NO_2	3.22	17.4	6.2	3.98	17.4	12.2	5.73	12.2	6.2	
s	H	2-NO_2	3.31	17.8	5.8	4.08	17.8	12.4	5.91	12.4	5.6	

The assignment of H_A and H_M signals was achieved by comparison of the corresponding experimental vicinal long-range coupling constant with H_X, namely, J_{AX} and J_{MX}, and comparison of the correlation of their DFT calculated dihedral angles (ϕ_1 = H_A–C_4–C_5–H_X and ϕ_2 = H_M–C_4–C_5–H_X in Fig 1) with the expected J values, considering the Karplus

equation [27]. According to this equation, the coupling constant is varied by changing the ϕ dihedral angle and is expected to increase by going from $\phi = 90^{o}$ towards either $\phi = 0^{o}$ or 180^{o}. Therefore, a larger coupling constant (J_{MX}) is expected for spin-spin coupling between the H_M and H_X protons as compared to that between the H_A and H_X protons (J_{AX}), namely, H_A is *cis*-orientated towards the C_5-aryl substituent (i.e. H_A is *trans*-orientated towards the H_X). The spectral data presented in Table 3 indicate that, as expected, the coupling constants are not varied drastically by changing the electronic nature and positions of the additional substituents either on the C_3- or C_5-aryl ring, whereas the electronic and steric effects of these substituents influence the characteristic chemical shifts of protons of this AMX system.

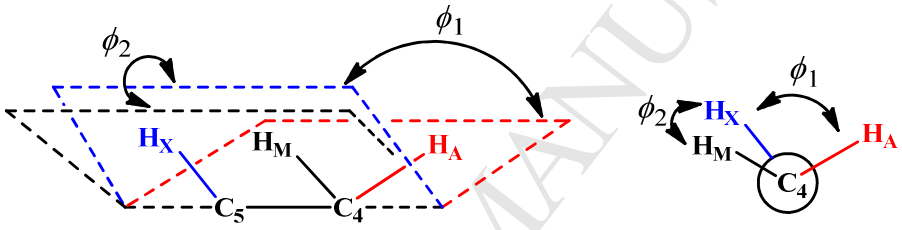

Fig 1. The dihedral angles ϕ_1 = H_A-C_4-C_5-H_X and ϕ_2 = H_M-C_4-C_5-H_X defining the *J*-coupling in the AMX system corresponding to Karplus diagram in the structures of 2-pyrazolines (**1a-s**, Table 1).

In order to elucidate the steric and electronic effects of the additional substituent especially on the C_5-position on the experimental ^{1}H chemical shifts and corresponding coupling constants of the heterocyclic hydrogen atoms (AMX system), computational studies were carried out using density functional theory (DFT) B3LYP method with the 6-311++G(d,p) basis set. Results of these computations are reported in Table 4. Comparison of the ^{1}H NMR data of the methoxy substituted derivatives on the 4-, 3- and 2-positions of the C_3-aryl ring (**1h**, **1i** and **1j**) and on the C_5-aryl ring (**1k**, **1l** and **1m**) indicates that π-donor and σ-donor characters of the methoxy group on the chemical shift of C_5–H_x proton, compared to those in the parent compound **1a**, is not drastic and only in the case of 2-CH_3O group on the C_5-aryl position (**1m**), downfield shift of the H_x proton (C_5–H_x) from 5.48 to 5.62 ppm is

observed. DFT optimized structure of **1m** shown in Fig 2 indicates that due to the attachment of C_5 atom to the electronegative N_1 atom, the hydrogen atom in C_5–H_x bond is relatively more polarized than a normal C-H bond, and therefore, the oxygen atom of the 2-CH_3O group is orientated towards the C_5–H_x hydrogen atom because of significant electrostatic interaction resulting in a 2.4399 Å distance. This interaction partly explains the downfield shift of this H_x proton in **1m**.

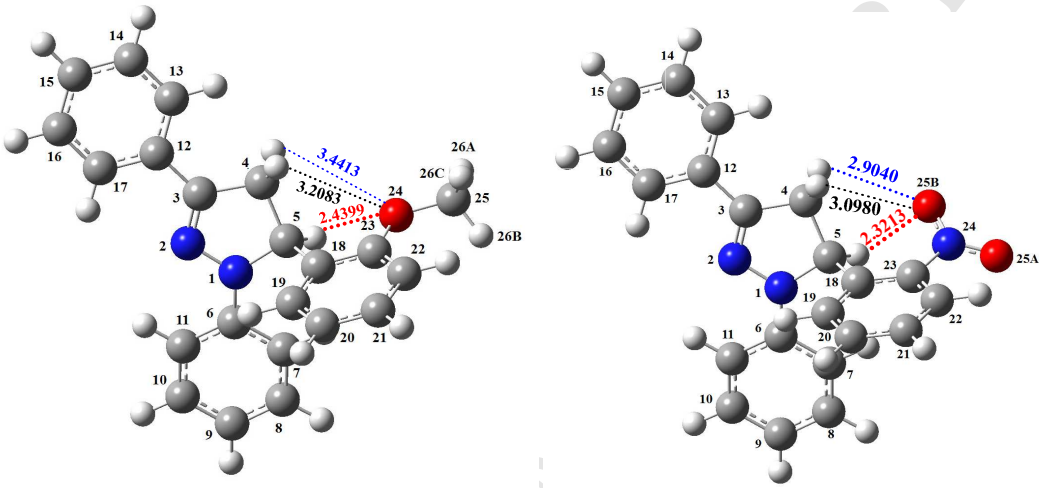

Fig 2. DFT optimized structures of **1m** (left) and **1s** (right) in DMSO (CPCM model solvent) showing the significant intramolecular electrostatic interactions between the hydrogen of the C_5–H_x bond and the oxygen atoms of the methoxy and nitro groups, respectively.

Comparison of the ^{1}H NMR data of the nitro-substituted derivatives on the 4-, 3- and 2-positions of the C_3-aryl ring (**1n**, **1o** and **1p**) and on the C_5-aryl ring (**1q**, **1r** and **1s**) indicates clearly the effective π- and σ-electron-withdrawing characters of nitro-substituted aryl ring changing the chemical shifts of all three hydrogen atoms of the heterocyclic ring, compared to those in the parent compound **1a**. The more effective downfield shift observed for the H_x proton (C_5–H_x) from 5.48 to 5.91 ppm in compound **1s**, having the NO_2 group on the *ortho*-position of C_5-aryl ring, is attributed to the intramolecular electrostatic interaction of one of the oxygen atoms of this nitro group with the hydrogen of the polarized C_5–H_X bond with a

distance of 2.3213 Å. In this compound, plane of the nitro group is deviated from ring co-planarity by 28.4º (as compared to 0.5º and 0.4º in **1q** and **1r**, respectively) to orient towards the H_x, H_A and H_M to have more effective interactions, as shown in Fig 2. In addition, the higher vibrational frequencies calculated for the C_5-H_x stretching for **1m** and **1s** as compared to that in the reference compound **1a** (see the IR section below) support the suggestion of the intramolecular electrostatic interaction of the methoxy and nitro substitutions at the *ortho*-position respectively in **1m** and **1s** with the hydrogen of C_5-H_X bond.

The electron-withdrawing inductive effect of the chlorine atom causes also downfield shift of the protons of the AMX system. The steric and electronic effects of the additional substituents on the C_3- and C_5-aryl groups on the *J*-coupling constants are explained considering results of the DFT computations reported in Table 4, to be compared with the corresponding experimental values reported in Table 3. These chemical shifts and *J*-coupling constants are calculated using the GIAO methods, respectively.

Table 4. The dihedral angles and the calculated chemical shifts and *J*-coupling constants for the AMX system obtained for 2-pyrazolines **1a-1s** in their B3LYP/6-311++G(d,p) structures optimized in the CPCM model solvent of DMSO

Comp.	δ_A	δ_M	δ_X	J_{AM}	ϕ_1	J_{AX}	ϕ_2	J_{MX}
1a	3.11	4.13	5.41	16.7	120.3	5.4	0.2	13.5
1b	3.07	4.07	5.42	16.7	120.3	5.4	0.2	13.5
1c	3.08	4.05	5.52	16.6	119.7	5.3	0.8	13.6
1d	4.00	3.87	5.42	17.0	135.1	9.8	14.8	12.6
1e	3.11	4.11	5.40	16.7	121.3	5.7	0.8	13.5
1f	3.14	4.13	5.34	16.7	123.1	6.1	2.6	13.5
1g	3.05	4.27	5.78	16.4	117.2	4.8	3.5	13.5
1h	3.07	4.09	5.30	16.7	123.4	6.3	2.8	13.3
1i	3.13	4.13	5.45	16.6	120.1	5.3	0.4	13.5
1j	3.09	4.60	5.46	17.6	114.2	3.9	6.5	13.5
1k	3.08	4.06	5.41	16.6	117.8	4.7	2.7	13.3
1l	3.11	4.10	5.38	16.7	124.7	5.3	4.2	13.5
1m	2.98	4.17	5.87	16.3	114.7	4.3	6.1	13.2

1n	3.13	4.05	5.66	16.5	117.3	4.9	3.2	13.6
1o	3.13	4.10	5.59	16.6	118.5	5.1	2.1	13.6
1p	3.07	3.50	5.63	16.7	115.7	4.5	5.1	13.4
1q	3.14	4.18	5.52	16.7	123.8	6.5	3.2	13.7
1r	3.13	4.19	5.52	16.8	120.9	5.6	0.3	13.6
1s	3.28	4.44	5.78	17.0	116.9	4.9	3.6	13.3

As can be seen in Table 4, the J_{MX} values are generally larger than the corresponding J_{AX} values because of larger distance of the ϕ_2 from 90º reference orientation as compared to the ϕ_1 dihedral angle, which is consistent with the Karplus diagram. These results shows that the vicinal *J*-coupling constants of the AMX spin system reflect the $H_{A/M}$-C_4-C_5-H_x dihedral angles which is determined by nature and position of the substituent on the C_3- and C_5-aryl rings. Furthermore, the steric hindrance of the substituent on the 2-position of these aryl rings has the most significant effect on the J_{AX} and J_{MX} values. Finally, comparative analysis shows that variation trends of the experimental (Table 3) and calculated (Table 4) chemical shifts with the substituents on the C_3- and C_5-aryl rings are similar.

After examining the NMR spectra, it was found out that in some derivatives, the substituent effects on the proton chemical shifts are not as expected. In addition to the important factors including inductive, resonance and through space (field) effects used usually to describe the substituent effects, the aromatic current ring, changed by the nature and position of the additional substituent, is also another significant factor affecting the NMR characteristics. Specifically, for the H_A, H_M and H_X protons of the AMX system described above, which are close to the C_5-aryl ring, this ring current can contribute to the NMR chemical shifts of these protons through space depending on the orientation of this aryl ring relative to the heterocyclic ring. To investigate this contribution, the (NICS) induced by this ring current is calculated for a point (Bq) located 0.5 Å above the center of the C_5-aryl ring in

the B3LYP/6-311++G(d,p) optimized structures (Fig 3) of a selected set of derivatives using (IGAIM) method.

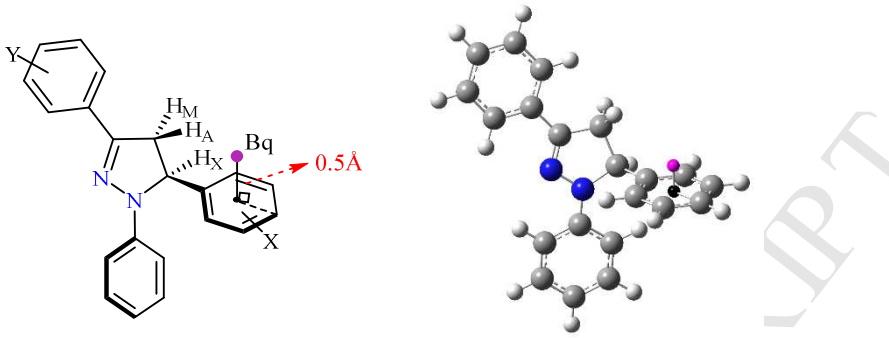

Fig 3. Position of the Bq point for which the NICS is calculated for this family of compounds (left) and in the optimized structure of **1a** as representative (right).

The calculated NICS values are presented in Fig 4 where they have been compared with the corresponding calculated and experimental chemical shifts of the AMX system protons. A complete correlation between variations of the NICS values at the Bq site and the chemical shifts of a specific proton denotes important contribution of the ring current to these chemical shifts. It is basically not possible to isolate the effects of each inductive, resonance, field and ring current contributions, since chemical shift is determined by collective effects of these factors which depend differently on the nature and position of the additional substituents. For the specific Bq point selected in this NICS analysis, an upfield shift in the NICS value correspond to an opposite (downfield) shift in the chemical shift of the protons located in-plane with the aryl ring. Therefore, the negative sign of the NICS values are omitted in Fig 4. As can be seen from this Fig, the calculated chemical shifts of the H_x proton has the best correlation with the NICS at the Bq point due to the closer position to the C_5-aryl ring and stronger feeling of its ring current. While, the H_A and H_M protons show weaker correlation because of their farther positions from this ring. Comparison of the AMX system calculated chemical shifts in the methoxy-substituted C_5-aryl ring (**1k**,**1l**,**1m**) shows that chemical shifts

of the AMX protons of compound **1m** have the least match with the NICS value at the Bq point, which can be attributed to their farther positions from co-planarity with the C_5-aryl ring (e.g. compare the H_X-C_5-C_{18}-C_{23} dihedral angels 26.8°, 27.5° and 39.4° for the **1k**, **1l** and **1m**, respectively). Interaction between the methoxy O atom and the H_X proton, described above in Fig 2, partially cancels this effect of relative orientation in the **1m** compound. Among 2-pyrazolines **1q**, **1r** and **1s**, having nitro-substitution on different positions of the C_5-aryl ring, the best agreement between the NICS values and the calculated chemical shifts belongs to the **1s** compound in the order of $H_A > H_M > H_X$. These trends, which are opposite to what observed for the methoxy-substituted derivatives **1k**, **1l** and **1m**, can be explained in terms of the smaller difference between the relative orientations of the AMX system with the C_5-aryl ring (e.g. note the calculated dihedral angles H_X-C_5-C_{18}-C_{23} 28.9°, 28.0° and 32.7° for the **1q**, **1r** and **1s**, respectively) and stronger donor-acceptor interactions between the oxygen atom of the nitro group and the AMX protons in the strength order of $H_A < H_M < H_X$ based on the O-H distances labeled in Fig 2. These evidences denote diminished effect of the current ring for this series of compounds compared to the local interactions.

A comparative analysis of the experimental and computational chemical shifts presented in Fig 4, shows evidently that trends observed for the variations of these two sets of chemical shifts for the methoxy- and nitro-substituted C_5-aryl ring (as in **1k**, **1l**, **1m** and **1q**, **1r** and **1s** derivatives) are similar. The compatibility of the calculated ^{1}H NMR chemical shifts obtained in the presence of the CPCM model solvent of DMSO is much better than that of obtained in the gas phase.

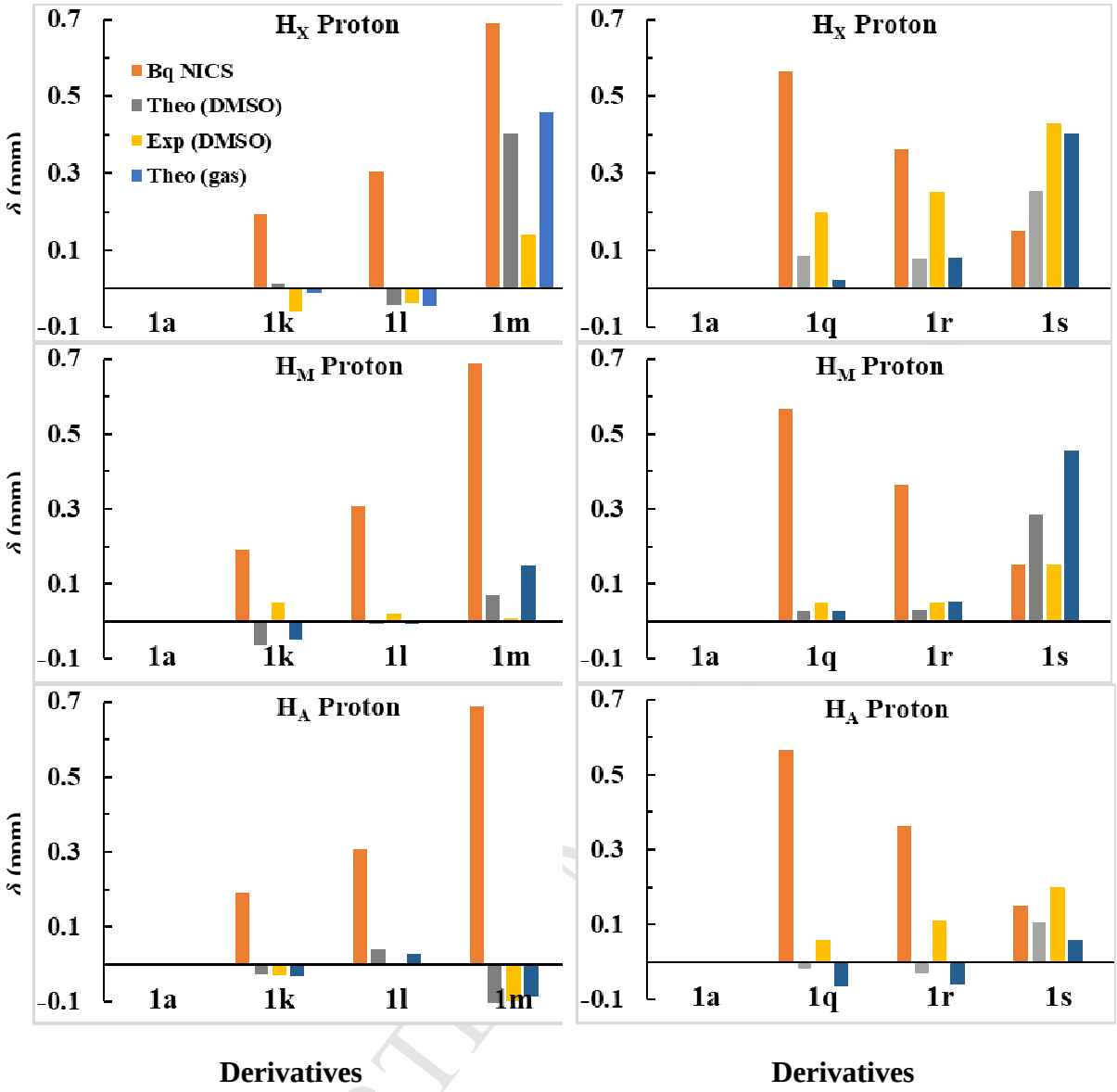

Fig 4. The IGAIM NICS values calculated at the point Bq (Fig. 3) for selected C_5-aryl substituted 2-pyrazolines, methoxy derivatives **1k**, **1l**, and **1m** (left column) and nitro derivatives **1q**, **1r**, and **1s** (right column), compared to the corresponding calculated and experimental chemical shifts of the AMX protons (Fig. 1 and 2). All values are referenced with respect to those of the unsubstituted 2-pyrazoline (**1a**). The data obtained computationally in the gas phase are also presented for comparison.

3.2. UV-Vis Study

Electron-donor acceptor abilities of the substituted aryl rings on the 3- and 5-positions of the heterocyclic ring were investigated by UV-Vis spectroscopy. The UV-Vis spectra of 2-

pyrazolines **1a-s** were obtained in $CHCl_3$ and the characteristic UV-Vis absorptions are presented in Table 5.

Table 5. Important electronic UV-Vis absorptions obtained experimentally for the aryl substituted 1-phenyl-2-pyrazolines (**1a-s**, scheme 1) in $CHCl_3$

1	Y	X	λ_{max} (log ε) in nm
a	H	H	355 (4.32), 313 (sh, 3.96), 241 (4.30)
b	4-Cl	H	367 (4.36), 315 (sh, 3.92), 243 (4.31)
c	3-Cl	H	367 (4.34), 312 (sh, 3.84), 246 (4.22)
d	2-Cl	H	357 (4.19), 314 (sh, 3.89), 246 (4.13)
e	H	4-Cl	355 (4.26), 242 (4.23)
f	H	3-Cl	356 (4.28), 316 (sh, 3.97), 240 (4.21)
g	H	2-Cl	355 (4.25), 316 (sh, 3.92), 240 (4.19)
h	4-CH_3O	H	354 (4.17), 321 (sh, 3.97), 250 (4.16)
i	3-CH_3O	H	360 (4.27), 241 (4.12)
j	2-CH_3O	H	357 (4.34), 251 (4.28)
k	H	4-CH_3O	357 (4.29), 315 (sh, 3.95), 239 (4.27)
l	H	3-CH_3O	356 (4.22), 241 (4.17)
m	H	2-CH_3O	360 (4.27), 315 (sh, 3.92), 243 (4.24)
n	4-NO_2	H	446 (4.35), 267 (4.21)
o	3-NO_2	H	354 (4.17), 321 (sh, 3.97), 250 (4.16)
p	2-NO_2	H	350 (4.13), 296 (sh, 3.96), 246 (4.27)
q	H	4-NO_2	350 (4.31), 249 (4.32)
r	H	3-NO_2	351 (4.20), 247 (4.26)
s	H	2-NO_2	353 (4.36), 313 (sh, 4.09), 243 (4.36)

The nature of the substituents considered in the present study, compared to the phenyl-substituted parent compound **1a**, is classified as strong electron-donating or activating (CH_3O group), strong electron-withdrawing or deactivating (NO_2 group) and weak deactivating but electron-donating (chlorine atom) substituents. As is mentioned earlier, the substituted aryl ring can be considered as a σ-donor or as a σ-acceptor substituent due to its attachment to the sp^3 hybridized carbon atom, namely, C_5-position of the heterocyclic ring, while these substituents themselves can possibly behave as π-donor or π-acceptor substituent due to the attachment to the sp^2 hybridized carbon atom of the C_3-position. Comparison of the UV-Vis spectral data (Table 5) of 2-pyrazolines containing chlorine atom on the 4-, 3- and 2-positions either of the C_3-aryl ring (**1b**, **1c** and **1d**) or of the C_5-aryl ring (**1e**, **1f** and **1g**) indicates that the maximum absorption wavelengths for **1d**, **1e**, **1f** and **1g** do not differ from that of **1a**. The observed bathochromic shift in the absorption peaks of compounds **1b** and **1c** (of ca. 10 nm) compared to that of **1a** and other chlorine containing compounds can be possibly due to the electron donating of the *para*- and *meta*-substituted C_3-aryl ring towards the electron-withdrawing imine bond (C=N) of the heterocyclic ring, which changes the spacings between the HOMOs and LUMOs energy levels contributing to the UV transitions. The observed lower wavelength of the absorption peak of **1d** (at 357 nm), compared to those of the two corresponding compounds **1b** and **1c** (at 367 nm), can be attributed to the non-coplanar orientation of the 2-chlorophenyl and heterocyclic rings due to steric hindrance of the chlorine atom with CH_2 moiety, which is approved by the results of B3LYP/6-311++G(d,p) computations carried out in the chloroform CPCM solvent. Comparison of the optimized value of the dihedral angle $\alpha = N_2\text{-}C_3\text{-}C_{12}\text{-}C_{13}$ in **1d** (154.1°) with those in **1b** (177.7°) and **1c** (178.6°) supports this suggestion. This is while, almost identical UV-Vis spectrum obtained for the **1e**, **1f** and **1g** compounds (Fig 5) indicates that the chlorophenyl substitution at the C_5-position has no significant effect on the UV-Vis transitions since these

substitutions contribute to the electronic structure of compound only via the σ-bond. These observations and justifications are approved by the calculated UV-Vis transition energies and spectra which are reported in Table S2 of the Supporting Information. For these calculations time-dependent density functional theory (TD-DFT) B3LYP/6-311++g(d,p) method considering 10 excited states is used in the presence of chloroform CPCM solvent in accordance with the experimental conditions. Computations show also that the chloro substitution on the C_3-aryl ring in **1b** and **1c** lowers both HOMO and LUMO energies as compared to those of the parent compound **1a**, such that their HOMO-LUMO energy spacings (see Table S2 of the Supporting Information) are reduced and thus results in an increase in their maximum absorption wavelengths.

Interestingly, comparison of the UV-Vis spectra (Fig 5) of the *para*-substituted chlorophenyl group on the C_3- and C_5-positions, respectively in **1b** and **1e**, with that of **1a,** indicates that the σ-donor ability of *para*-chlorophenyl substituent in **1e** does not affect its maximum absorption as opposed to the significant red shift observed for **1b** due to its π-donor ability. The weak σ-donor ability of the chlorophenyl substituent on the C_5-position is also supported by obtaining almost the same UV-Vis absorption spectra for **1e**, **1f** and **1g**, (Fig 5) having the chlorine atom respectively on the *para-*, *meta-* and *ortho*-positions on the C_5-aryl ring (Table 5).

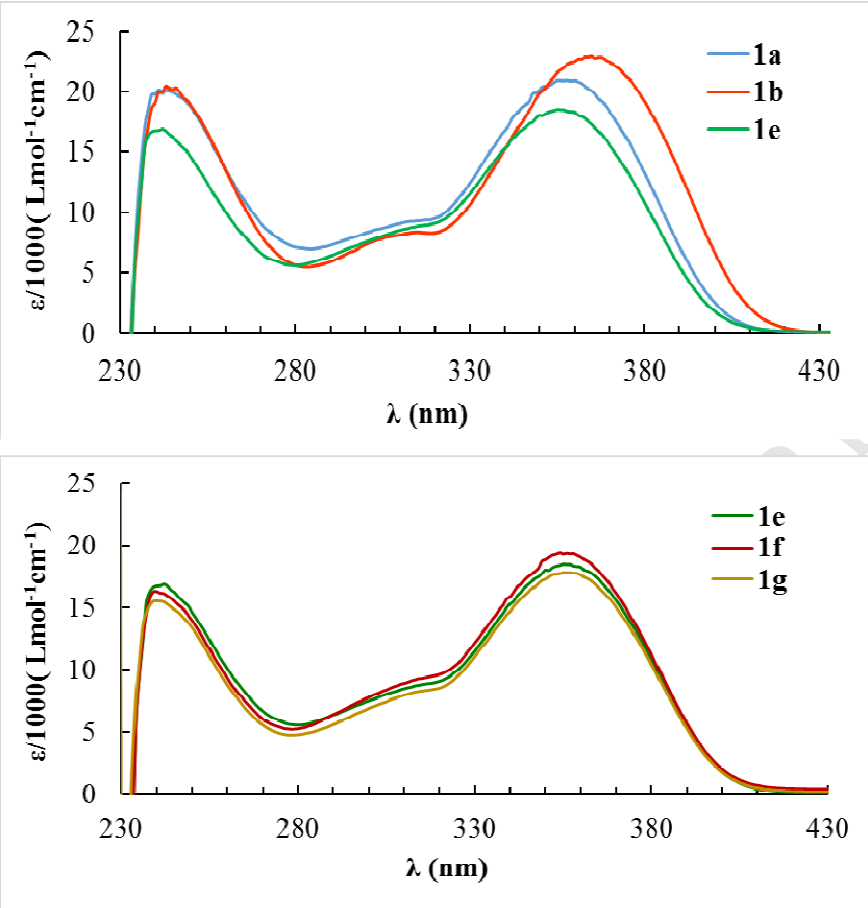

Fig 5. Comparison of the UV-Vis spectra of **1b** and **1e** containing 4-chlorophenyl substituted C_3- and C_5-aryl rings with that of **1a** showing the π-donor ability of the group in **1b** *versus* its σ-donor ability in **1e** (a). Almost identical UV-Vis spectra obtained for the **1e**, **1f** and **1g**, are shown in (b).

Maximum UV-Vis absorptions of the methoxyphenyl-substituted 2-pyrazolins on the C_3- (**1h**, **1i** and **1j**) and C_5-positions (**1k**, **1l** and **1m**) are given in Table 5. Comparison of their UV-Vis spectra with that of the parent compound **1a** indicates that the difference between the π- and σ-donor abilities of the methoxyphenyl substitutions is not drastic. This supports the suggestion that the heterocyclic ring is not an electron-accepting group against the methoxyphenyl group.

Interesting trends have been observed by comparison of the maximum UV-Vis absorptions of the **1n**, **1o** and **1p** (with *para*-, *meta*- and *ortho*-nitrophenyl substituents at C_3-

position), and **1q**, **1r** and **1s** (with *para*-, *meta*- and *ortho*-nitrophenyl substituents at C_5-position) shown in Fig 6.

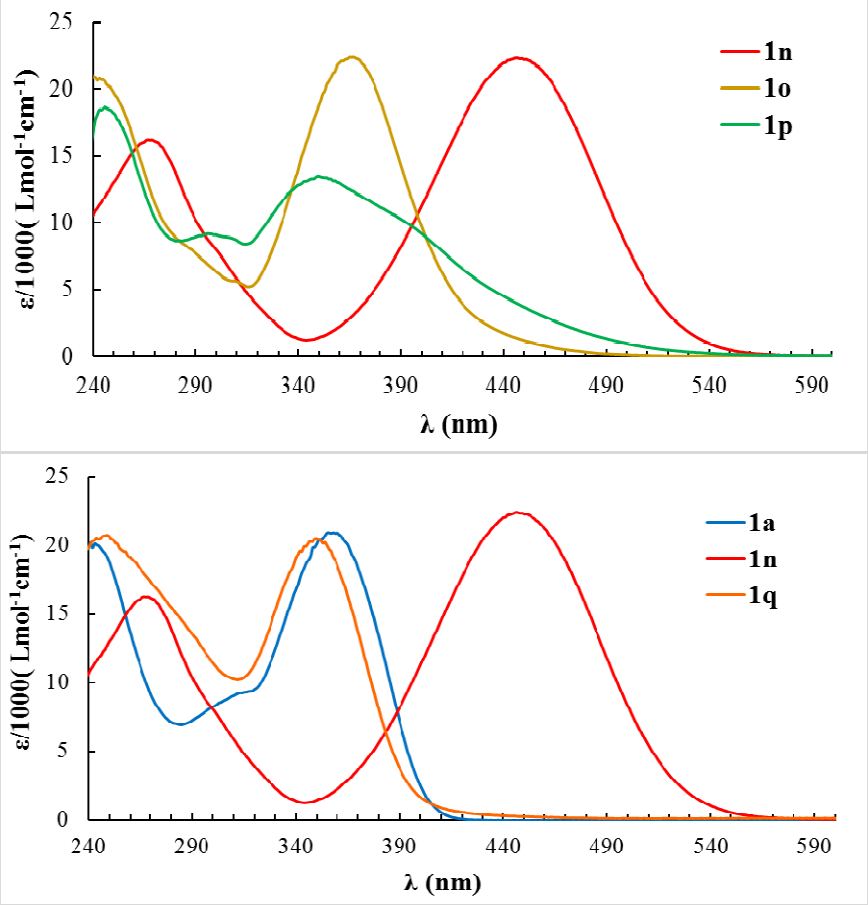

Fig 6. Comparison of the experimental UV-Vis absorption spectra of **1n**, **1o** and **1p** containing respectively *para*-, *meta*- and *ortho*-nitrophenyl group on the C_3-position of the heterocyclic ring, (top), and of C_3- and C_5-*para*-nitrophenyl substituted 2-pyrazolines with that of **1a** (bottom).

The observed bathochromic shift of the UV-Vis absorption peak of **1n** is explained by *through conjugation* of the lone pair on the N_1-atom of the heterocyclic ring towards the electron-withdrawing NO_2 group at the *para*-position of the C_3-aryl ring. It is basically expected that the co-planar orientation of the electron-pulling NO_2 group on the *ortho*- and *para*-positions, either on C_3- or C_5-aryl rings, results in the induction of the positive charge on the C-atom of the aromatic ring attached to the C_3- or C_5-atoms of the heterocyclic ring.

Whereas the electron-withdrawing effect of this group on the C_5-position *via* the σ bond (C_{18}-C_5 bond) decreases the electron-donating ability of the heterocyclic ring, co-planar orientation of the C_3-aryl ring with the C_3=N_2 double bond allows effective delocalization of the lone pair of the N_1-atom towards the positive charge in the proposed resonance structure illustrated in Fig 7, which we will assign as *through conjugation* from the N_1-lone pair towards the electron-pulling NO_2 group either on the *ortho*- or *para*-position. This is indicated by appearance of the intensive color and the effective visible light absorption of compound **1n** as shown in Fig 7. The effective and strong π-electron pulling effect of the *para*-nitrophenyl group on the C_3-position (compound **1n**) *versus* its weak σ-electron pulling effect on the C_5-position (compound **1q**) can be deduced from the UV-Vis absorption peaks shown in Fig 6.

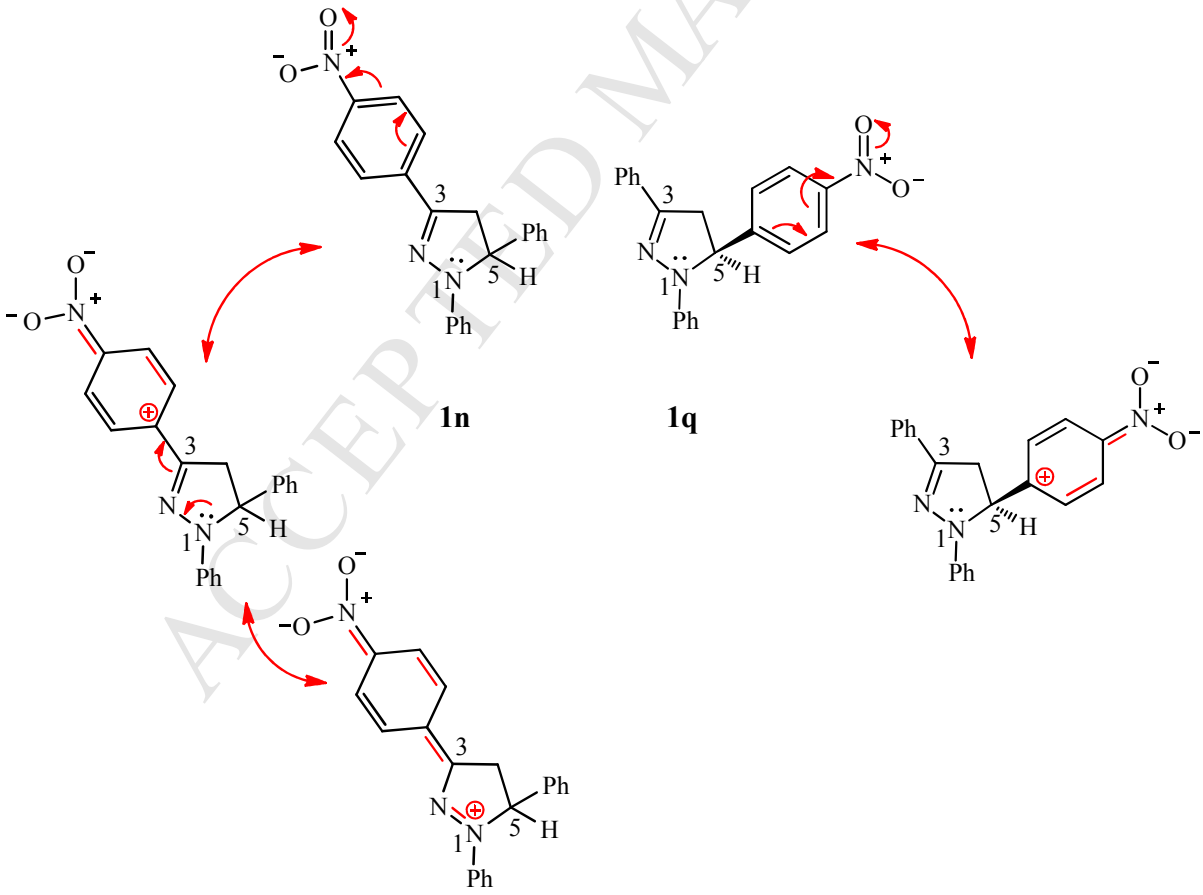

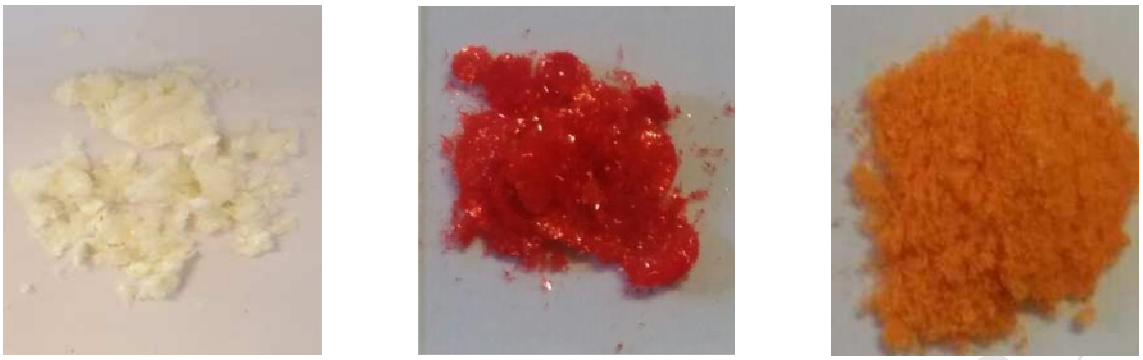

1a **1n** **1q**

Fig 7. The observed *through conjugation* from N_1-lone pair towards the *para*-nitrophenyl group on the C_3-position in **1n** causes effective visible light absorption compared to that in **1q** and the parent compound **1a**.

Surprisingly, a comparison of the UV-Vis absorption of the *para*- and *ortho*-nitrophenyl substituted compounds **1n** and **1p** does not show effectively the *through conjugation* in compound **1p**. As can be seen in Table 5 and Fig 6, position of the UV absorption peak (at 350 nm) of compound **1p** does not significantly differ from that of parent compound **1a** (at 355 nm). This can be attributed to the special non-co-planar inter-ring (α dihedral angle) and NO_2–ring (θ dihedral angle) conformations adopted in this compound (computed respectively to be α = 149.6° and θ = –34.1° dihedral angles, as defined in Fig 8) prevents *through conjugation* from the heterocyclic ring nitrogen atom to the NO_2 group, which does not allow the NO_2 group to act as an effective π-acceptor, while still acting as a σ-acceptor. Therefore, the UV peak of **1p** resembles that of **1o** in which the nitro group in the *meta*-position acts also as a σ-acceptor.

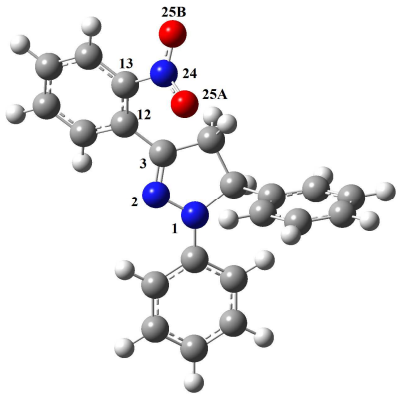

α =149.6 °	θ = –34.1°

Fig 8. The optimized conformation of the **1p** compound showing the orientation of the C_3-aryl ring with respect to the heterocyclic ring (defined by the dihedral angle α = N_2-C_3-C_{12}-C_{13}) and the orientation of the NO_2 substitution with respect to the C_3-aryl ring plane (defined by the dihedral angle θ = O_{25A}-N_{24}-C_{13}-C_{12}).

The tendency of the heterocyclic ring towards the C_3-substituted aryl ring of different natures, namely, the electron-donating *para*-methoxy group in **1h** *versus* the electron-withdrawing *para*-nitro group in **1n** was elucidated by comparison of the experimental and calculated UV spectra with those of the parent compound **1a** (Fig 9). A detailed analysis of the two sets of UV-Vis spectra (Tables 5 and S3-S5) shows a close correlation between the experimental and computational UV-Vis absorption wavelengths (energies), although the numerical values of the two sets are not exactly compatible. The differences between these values can be attributed mainly to the well-known gas-to-liquid shift due to specific, mainly solute-solvent, interactions in the form of electrostatic and hydrogen bonding [28], in addition to the limitations and approximations of the theoretical method used in our calculations. Based on the data reported in Tables S3-S5, the theoretical and experimental absorption wavelengths are in relatively good agreement for the **1a** and **1h**, but not for the **1n** compound. Also, the differential wavelengths of the two peaks in the theoretical spectra, $\Delta\lambda_{max}(theo) = \lambda_{max1}(theo) - \lambda_{max2}(theo)$, and in the experimental spectra, $\Delta\lambda_{max}(exp) = \lambda_{max1}(exp) - \lambda_{max2}(exp)$, for the **1n** compound is larger (40.6 nm) than those for the **1a** (17.5 nm) and **1h**

(12.8 nm) compounds. This can be attributed to the more profound solvent effect for the **1n** compound due to its stronger electrostatic interactions with the solvent which is approved by its larger calculated dipole moment (9.3064 Debye) as compared to the smaller dipole moments of **1a** and **1h** (3.6129 and 2.7832 Debye, respectively). The preferred delocalization of the N_1 lone pair towards the C_3-aryl ring allows the occurrence of the resonance structure type **RS-I** (Scheme 3), which is more stabilized by the electron-withdrawing resonance effect of the nitro group on the 4-position illustrated in Fig 7. These suggestions are supported by larger calculated dipole moment for this compound mentioned above, and consequently, higher solute/solvent interaction for **1n** is expected. Computations with the explicit solvent molecules can greatly improve theoretical results but is not intended in this work. However, the TD-DFT computations have reproduced fairly well comparative intensities of the UV-Vis peaks, and even the shoulders of the UV-Vis spectra demonstrated in Fig 9.

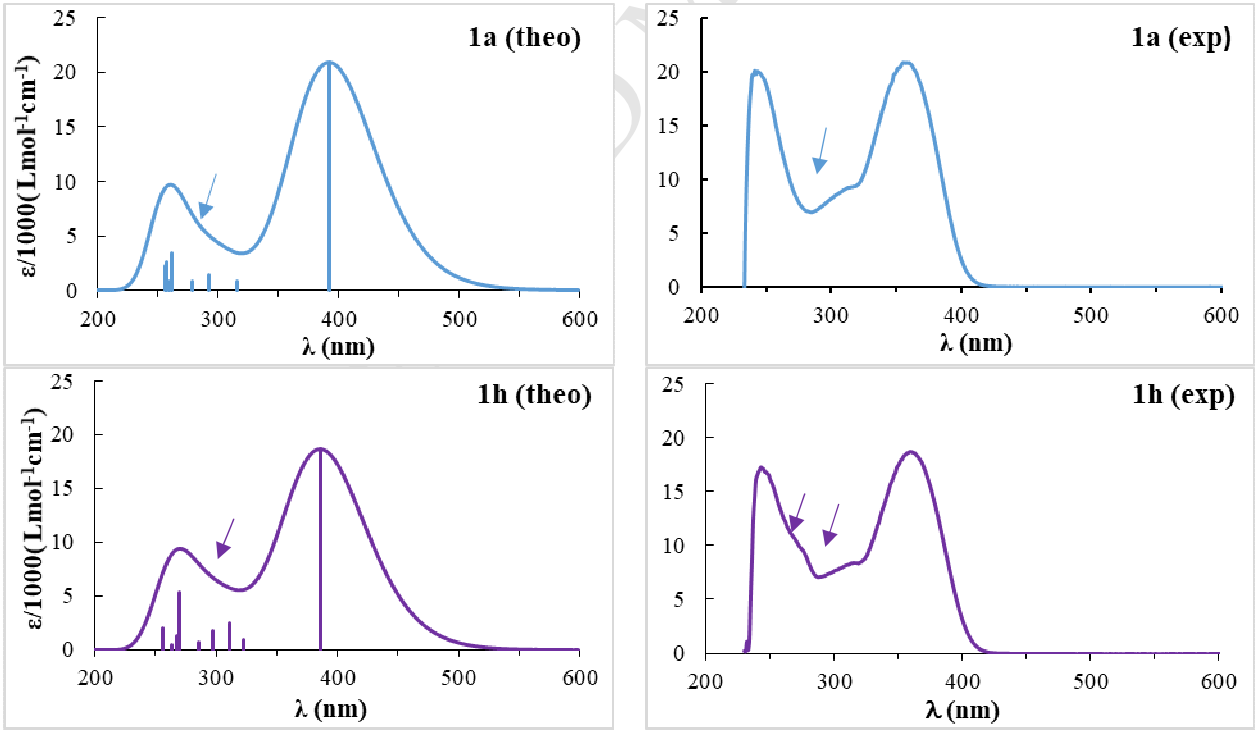

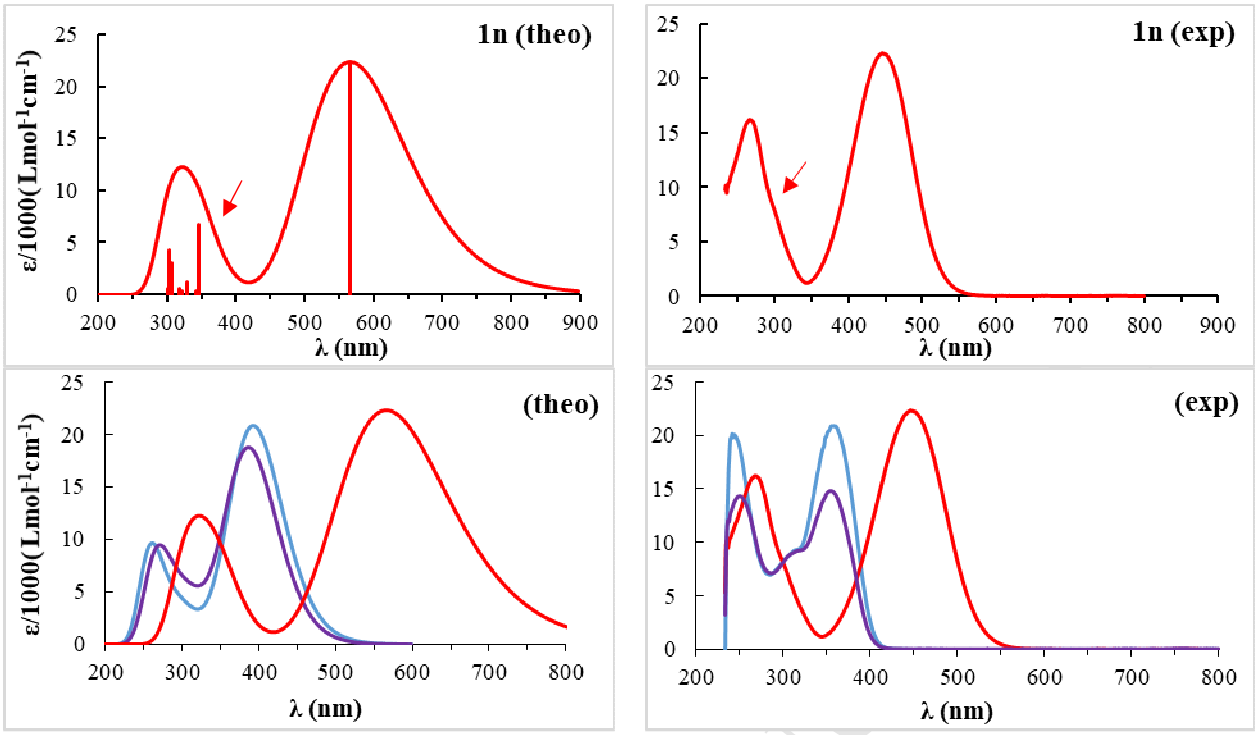

Fig. 9. The computational (left) and experimental (right) UV-Vis absorption spectra of **1a**, **1h** and **1n** in $CHCl_3$, showing the effects of the $–OCH_3$ and $–NO_2$ groups on the *para*-position of the C_3-aryl ring of the 2-pyrazolines studied in this work. The arrows, pointing the shoulders, show further agreement of the calculated and experimental spectra. In the lowest row, all these UV-Vis spactra are plotted together for better comparison.

3.3. IR Study

The infrared spectra of the 2-pyrazolines **1a-s** have been obtained and the main stretching bands are assigned and presented in Tables S6-S9 in the Supplementary Information. Analysis of these experimental IR bands [29] reflect the resonance and inductive effects of the substituents, which is more remarkable for some derivatives. For example, the C=N stretching frequency in **1a**, **1h** and **1n** compounds are respectively 1596 cm^{-1}, 1600 cm^{-1} and 1593 cm^{-1} (Fig 10, left column), which denote the presence of *through conjugation* in **1n** compound due to the electron-withdrawing resonance effect of 4-nitro group *versus* electron-donating nature of 4-methoxy group in **1h** compared to that in **1a**. This conjugation can also be deduced by comparing the $C_3=N_2$ & N=O (nitro) and C_5-N_1 & C_5-H_X stretching frequencies of the four **1a**, **1n**, **1o** and **1p** compounds, which are respectively the lowest and

highest for **1n** (Fig 11). The observed shifts of the corresponding C_5-H_X bands in the **1n** compound to higher frequencies, is explained by the effective *through conjugation* in the proposed resonance structure described in Fig 7, results in a positive charge on the N_1-atom of the heterocyclic ring which leads to stronger C_5-N_1 and C_5-H_X bonds *via* induction effect. In addition, the B3LYP/6-311++G(d,p) calculated higher vibrational frequencies of the C_5-H stretching for **1m** (at 3076.43 cm^{-1}) and **1s** (at 3097.90 cm^{-1}) as compared to that in the reference compound **1a** (at 3042.67 cm^{-1}) (Fig 10, right column) support the suggestion of the intramolecular electrostatic interaction of the *ortho*-substitution in **1m** and **1s** with the H_X hydrogen atom of the C_5-H_X bond, as discussed in the NMR section above.

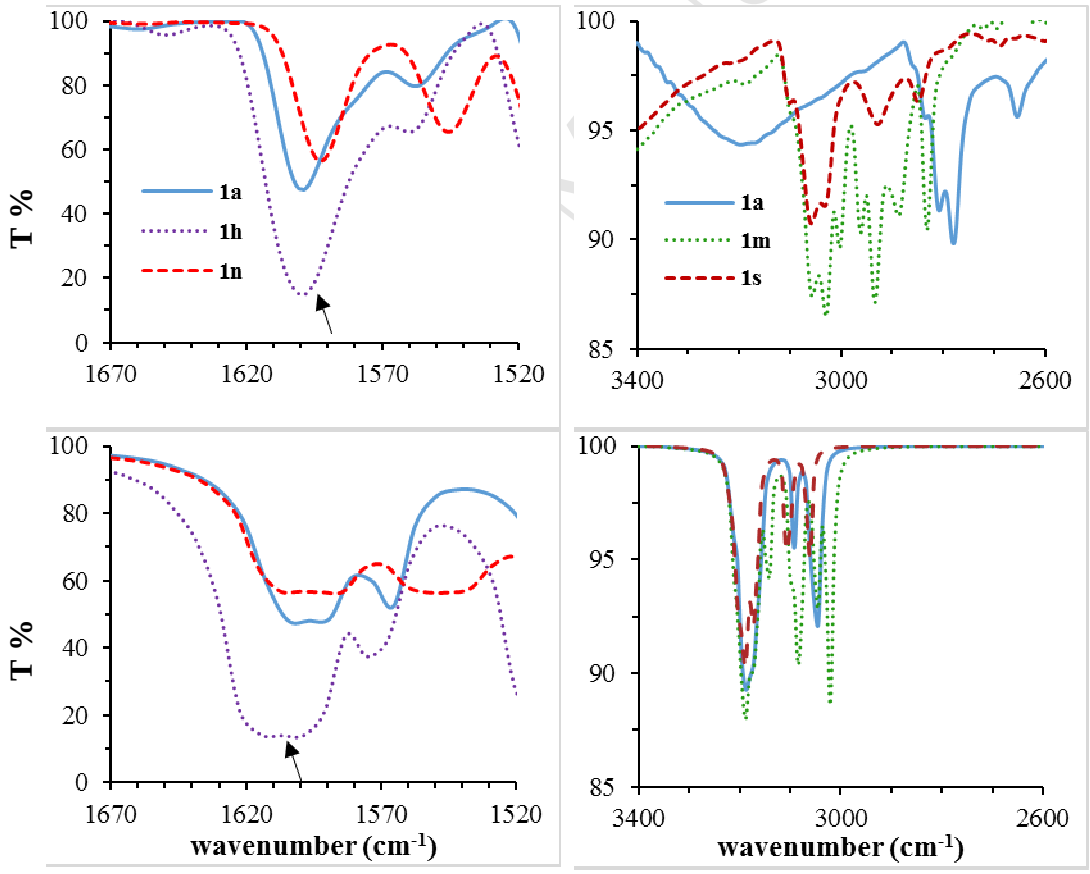

Fig. 10 The experimental (top row) and computational (bottom row) IR spectra obtained for **1a**, **1h** and **1n** (left column) and **1a**, **1m** and **1s** (right column), showing the effects of the CH_3O and NO_2 groups on the *para*-position of the C_3-aryl ring and on the *ortho*-position of the C_5-aryl ring of the 2-pyrazoline structure (Table 1).

Since, the C=N stretching bands for the (**1a**, **1m** and **1s**) and C-H streching bands for the (**1a**, **1h** and **1n**) sets of compounds are similar, the corresponding regions are not shown.

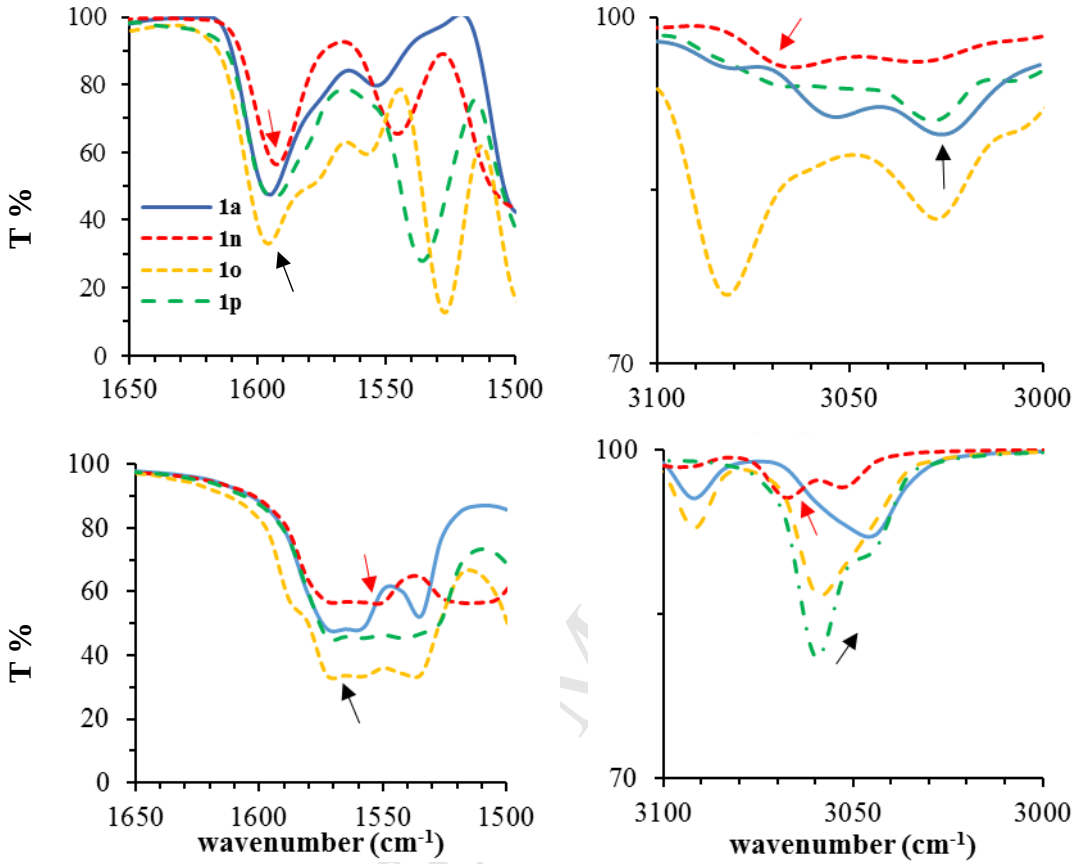

Fig. 11 The experimental (top row) and computational (bottom row) IR spectra obtained for **1a**, **1n**, **1o** and **1p** showing the effects of the NO_2 group on the *para*-, *meta*- and *ortho*-positions of the C_3-aryl ring of the 2-pyrazoline structure (Table 1) on the C_3=N_2 stretching bands and C_5-H_X streching bands for these compounds.

The broad bands appearing at the highest frequency of the experimental IR spectra (Fig 10) which are assigned to the stretching vibrations of the C-H bonds of the three aryl rings, denote variations of the orientations and inter-molecular interactions experienced by these aryl rings in the bulk of solid sample milled and dispersed in the KBr tablet. These variations of the electronic environment are not included in the DFT computations, and thus such a broad band is expected to be missing in the computed IR spectra, as can be seen in Fig 10. It

should also be noted that these non-bonding interactions shifts the corresponding C-H bands of the aryl rings to higher frequencies. Therefore, the structures of the C-H band regions in the two experimental and computational IR spectra are not expected to be so compatible, as is evident from Fig 10.

4. Conclusion

Steric and electronic effects of different electron-donating and electron-withdrawing substituents on the *ortho*-, *meta*- and *para*-positions of C_3-/C_5-aryl substituted 1-phenyl-2-pyrazolines were investigated by ^{1}H NMR, UV-Vis and IR spectroscopies. Analysis of the ^{1}H NMR chemical shifts obtained experimentally shows relatively good agreement with the GIAO ^{1}H NMR chemical shifts calculated for the B3LYP/6-311++G(d,p) optimized structures which depend on the variation of the electronic environment induced by the substitution. Also, the measured values of $^3J_{HH}$ are justified based on the Karplus analysis on the HCCH dihedral angles in the B3LYP/6-311G++G(d,p) optimized structures which is determined by the nature and position of the substitution. Furthermore, the calculated values of the nuclear independent chemical shift (NICS) indicate that in addition to the inductive, resonance and field effects, the ring current which is partly affected by the substituents, contributes to the ^{1}H NMR chemical shifts. The results of TD-DFT studies and experimental investigations are consistent and show that the UV-Vis spectra is affected mainly by the presence of the substituent on the C_3-aryl ring due to its π-donor/acceptor nature. This observation is more pronounced in **1n**, compound with a 4-nitro substitution on the C_3-aryl, for which the UV-Vis peak shows more significant red shift compared to that of **1q** compound, having a 4-nitro substitution on the C_5-aryl ring. Interestingly, in spite of the fact that the NO_2 group on both *para*- and *ortho*-positions of the C_3-aryl ring is expected to act as π-acceptor substituent, the UV-Vis absorption wavelengths of **1n** and **1p** compounds are significantly different. This can be attributed to the non-co-planar inter-ring and NO_2–ring

conformations when NO_2 group is on the *ortho*-position in **1p**, which consequently reduces the π-acceptor character of the C_3-aryl ring and therefore does not induce significant red shift compared to that of **1n**.

Intramolecular electrostatic interaction of the 2-CH_3O- and 2-NO_2- substitutions on the C_5-aryl ring with the C_5-H_x hydrogen atom in **1m** and **1s** compounds are discussed based on the analyses of both experimental and computational NMR chemical shifts and IR frequencies. As a final conclusion, substitutions on the C_3- and C_5-aryl rings affect differently the spectral characteristics and thus chemical properties of these 2-pyrazolines.

Appendix: Physical and spectroscopic data obtained for 2-pyrazolines

*1,3,5-Triphenyl-2-pyrazoline (**1a**)*

M.P. 134-136 ºC. IR (KBr): ν = 3057, 3026, 1596, 1554, 1498, 1451, 1392, 1327, 1267, 1124, 1070, 873, 758 cm^{-1}. ^{1}H NMR (400 MHz, DMSO-*d6*): δ = AMX-system, δ_A = 3.11 (J_{AM} = 17.6 Hz, J_{AX} = 6.4 Hz, 1H, 4-CH), δ_M = 3.93 (J_{AM} = 17.6 Hz, J_{MX} = 12.4 Hz, 1H, 4-CH), δ_x = 5.48 (J_{MX} = 12.4 Hz, J_{AX} = 6.4 Hz, 1H, 5-CH), 6.69-6.73 (m, 1H, aromatic H), 6.99-7.01 (m, 2H, aromatic H), 7.13-7.17 (m, 2H, aromatic H), 7.23-7.45 (m, 8H, aromatic H), 7.74-7.76 ppm (m, 2H, aromatic H). ^{13}C NMR (100 MHz, DMSO-*d6*): δ = 42.95 (C4), 63.08 (C5), 112.90, 118.57, 125.67, 125.82, 127.38, 128.63, 128.68, 128.85, 128.98, 132.23, 142.53, 144.19, 147.15 ppm (aromatic C). UV ($CHCl_3$): λ_{max} (log ε) = 355 nm (4.32), 313 (sh, 3.96), 241 (4.30).

*3-(4-Chlorophenyl)-1,5-diphenyl-2-pyrazoline (**1b**)*

M.P. 148-150 ºC. IR (KBr): ν = 3063, 3028, 1595, 1553, 1497, 1454, 1385, 1319, 1244, 1127, 1087, 870, 744 cm^{-1}. ^{1}H NMR (400 MHz, DMSO-*d6*): δ = AMX- system, δ_A = 3.11 (J_{AM} = 17.2 Hz, J_{AX} = 6.4 Hz, 1H, 4-CH), δ_M = 3.91 (J_{AM} = 17.6 Hz, J_{MX} = 12.4 Hz, 1H, 4-CH), δ_x = 5.51 (J_{MX} = 12.4 Hz, J_{AX} = 6.4 Hz, 1H, 5-CH), 6.71-6.75 (m, 1H, aromatic H),

6.95-7.02 (m, 2H, aromatic H), 7.14-7.18 (m, 2H, aromatic H), 7.24-7.37 (m, 5H, aromatic H), 7.65 (d, J = 8.8 Hz, 2H, aromatic H), 7.76 ppm (d, J = 8.8 Hz, 2H, aromatic H). ^{13}C NMR (100 MHz, DMSO-*d6*): δ = 42.79 (4-C), 63.30 (5-C), 113.01, 118.79, 125.81, 127.28, 127.41, 128.65, 128.64, 128.97, 131.16, 133.04, 142.36, 144.00, 146.08 ppm (aromatic C). ^{1}H NMR (400 MHz, $CDCl_3$): δ = AMX- system, δ_A = 3.13 (J_{AM} = 17 Hz, J_{AX} = 7.4 Hz, 1H, 4-CH), δ_M = 3.83 (J_{AM} = 17.2 Hz, J_{MX} = 12.4 Hz, 1H, 4-CH), δ_x = 5.31 (J_{MX} = 12.4 Hz, J_{AX} = 7.2 Hz, 1H, 5-CH), 6.80-6.84 (m, 1H, aromatic H), 7.08-7.10 (m, 2H, aromatic H), 7.18-7.23 (m, 2H, aromatic H), 7.27-7.39 (m, 7H, aromatic H), 7.49-7.68 ppm (m, 2H, aromatic H). ^{13}C NMR (100 MHz, $CDCl_3$): δ = 43.43 (C4), 64.62 (C5), 113.45, 119.36, 125.86, 126.91, 127.70, 128.78, 128.98, 129.23, 131.31, 134.28, 142.38, 144.62, 145.56 ppm (aromatic C). UV ($CHCl_3$): λ_{max} (log ε) = 367 nm (4.36), 315 (sh, 3.92), 243 (4.31).

*3-(3-Chlorophenyl)-1,5-diphenyl-2-pyrazoline (**1c**)*

M.P. 129-131 ºC. IR (KBr): ν = 3086, 3036, 1596, 1568, 1500, 1453, 1394, 1324, 1263, 1132, 1025, 874, 745 cm^{-1}. ^{1}H NMR (400 MHz, DMSO-*d6*): δ = AMX- system, δ_A = 3.21 (J_{AM} = 17.6 Hz, J_{AX} = 6.4 Hz, 1H, 4-CH), δ_M = 3.99 (J_{AM} = 17.6 Hz, J_{MX} = 12.4 Hz, 1H, 4-CH), δx = 5.60 (J_{MX} = 12.4 Hz, J_{AX} = 6.4 Hz, 1H, 5-CH), 6.80-6.83 (m, 1H, aromatic H), 7.10-7.11 (m, 2H, aromatic H), 7.22-7.55 (m, 9H, aromatic H), 7.75-7.77 (m, 1H, aromatic H), 7.85-7.86 (m, 1H, aromatic H). ^{13}C NMR (100 MHz, DMSO-*d6*): δ = 42.64 (C4), 63.25 (C5), 113.08, 118.92, 124.22, 125.03, 125.83, 127.44, 128.22, 128.87, 128.99, 130.51, 133.51, 134.42, 142.29, 143.82, 145.80 ppm (aromatic C). UV ($CHCl_3$): λ_{max} (log ε) = 367 nm (4.34), 312 (sh, 3.84), 246 (4.22).

*3-(2-Chlorophenyl)-1,5-diphenyl-2-pyrazoline (**1d**)*

M.P. 122-125 ºC. IR (KBr): ν = 3064, 3034, 1595, 1567, 1495, 1454, 1430, 1378, 1309, 1229, 1118, 866, 762 cm^{-1}. ^{1}H NMR (400 MHz, DMSO-*d6*): δ = AMX- system, δ_A = 3.22

(J_{AM} = 17.4 Hz, J_{AX} = 6.2 Hz, 1H, 4-CH), δ_M = 4.05 (J_{AM} = 17.4 Hz, J_{MX} = 12.2 Hz, 1H, 4-CH), δ_x = 5.50 (J_{MX} = 12.2 Hz, J_{AX} = 6.2 Hz, 1H, 5-CH), 6.73-6.76 (m, 1H, aromatic H), 7.01-7.03 (m, 2H, aromatic H), 7.14-7.18 (m, 2H, aromatic H), 7.24-7.42 (m, 7H, aromatic H), 7.52-7.54 (m, *J* = m, 1H, aromatic H), 7.75-7.77 ppm (m, 1H, aromatic H). ^{13}C NMR (100 MHz, DMSO-*d6*): δ = 45.42 (4-C), 63.18 (5-C), 113.13, 118.99, 125.85, 127.27, 127.45, 128.87, 128.98, 129.78, 130.10, 130.84, 130.94, 142.19, 143.99, 145.44 ppm (aromatic C). UV ($CHCl_3$): λ_{max} (log ε) = 357 nm (4.19), 314 (sh, 3.89), 246 (4.13).

*5-(4-Chlorophenyl)-1,3-diphenyl-2-pyrazoline (**1e**)*

M.P. 131-133 ºC. IR (KBr): ν = 3061, 2920, 1593, 1564, 1496, 1448, 1391, 1329, 1277, 1127, 1092, 998, 743 cm^{-1}. ^{1}H NMR (400 MHz, $CDCl_3$): δ = AMX- system, δ_A = 3.13 (J_{AM} = 17.2 Hz, J_{AX} = 7.2 Hz, 1H, 4-CH), δ_M = 3.87 (J_{AM} = 17 Hz, J_{MX} = 12.2 Hz, 1H, 4-CH), δ_x = 5.28 (J_{MX} = 12.2 Hz, J_{AX} = 7 Hz, 1H, 5-CH), 6.80-6.85 (m, 1H, aromatic H), 7.06-7.08 (m, 2H, aromatic H), 7.20-7.25 (m, 2H, aromatic H), 7.29-7.44 (m, 7H, aromatic H), 7.73-7.76 ppm (m, 2H, aromatic H). ^{13}C NMR (100 MHz, $CDCl_3$): δ = 43.48 (C4), 63.88 (C5), 113.43, 119.39, 125.38, 125.78, 125.86, 127.36, 128.61, 128.72, 128.77, 129.00, l29.10, 129.36, 129.99 ppm (aromatic C). ^{1}H NMR (400 MHz, DMSO-*d6*): δ = AMX- system, δ_A = 3.12 (J_{AM} = 17.5 Hz, J_{AX} = 6.2 Hz, 1H, 4-CH), δ_M = 3.92 (J_{AM} = 17.5 Hz, J_{MX} = 12.2 Hz, 1H, 4-CH), δ_x = 5.52 (J_{MX} = 12.2 Hz, J_{AX} = 6.2 Hz, 1H, 5-CH), 6.72-6.75 (m, 1H, aromatic H), 6.99-7.01 (m, 2H, aromatic H), 7.15-7.19 (m, 2H, aromatic H), 7.31-7.45 (m, 7H, aromatic H), 7.74-7.76 ppm (m, 2H, aromatic H). ^{13}C NMR (100 MHz, DMSO): δ = 42.72 (C4), 62.37 (C5), 112.94, 118.74, 125.70, 127.83, 128.62, 128.75, 128.90, 128.95, 131.89, 132.12, 141.41, 144.02, 147.27 ppm (aromatic C). UV ($CHCl_3$): λmax (log ε) = 355 nm (4.26), 242 (4.23).

*5-(3-Chlorophenyl)-1,3-diphenyl-2-pyrazoline (**1f**)*

M.P. 106-108 ºC. IR (KBr): ν = 3063, 2919, 1595, 1494, 1447, 1392, 1329, 1271, 1131, 1071, 1001, 874, 747 cm^{-1}. ^{1}H NMR (400 MHz, DMSO-*d6*): δ = AMX- system, δ_A = 3.16 (J_{AM} = 17.6 Hz, J_{AX} = 6.4 Hz, 1H, 4-CH), δ_M = 3.92 (J_{AM} = 17.6 Hz, J_{MX} = 12.0 Hz, 1H, 4-CH), δ_x = 5.53 (J_{MX} = 12.4 Hz, J_{AX} = 6.4 Hz, 1H, 5-CH), 6.73-6.77 (m, 1H, aromatic H), 7.00-7.02 (m, 2H, aromatic H), 7.16-7.19 (m, 2H, aromatic H), 7.20-7.26 (m, 1H, aromatic H), 7.32-7.45 (m, 6H, aromatic H), 7.75-7.77 ppm (m, 2H, aromatic H). ^{13}C NMR (100 MHz, DMSO): δ = 43.23 (C4), 62.94 (C5), 113.41, 119.32, 125.03, 126.25, 127.94, 129.13, 129.30, 129.46, 131.49, 132.57, 133.97, 144.52, 145.49, 147.90 ppm (aromatic C). UV ($CHCl_3$): λmax (log ε) = 356 nm (4.28), 316 (sh, 3.97), 240 (4.21).

*5-(2-Chlorophenyl)-1,3-diphenyl-2-pyrazoline (**1g**)*

M.P. 134-136 ºC. IR (KBr): ν = 3059, 2916, 1592, 1562, 1497, 1469, 1394, 1335, 1266, 1139, 1035, 875, 750, 689 cm^{-1}. ^{1}H NMR (400 MHz, DMSO-*d6*): δ = AMX- system, δ_A = 3.09 (J_{AM} = 17.4 Hz, J_{AX} = 6.3 Hz, 1H, 4-CH), δ_M = 4.02 (J_{AM} = 17.6 Hz, J_{MX} = 12.4 Hz, 1H, 4-CH), δ_x = 5.69 (J_{MX} = 12.2 Hz, J_{AX} = 6.2 Hz, 1H, 5-CH), 6.73-6.77 (m, 1H, aromatic H), 6.92-6.94 (m, 2H, aromatic H), 7.10-7.12 (m, 1H, aromatic H), 7.17-7.45 (m, 7H, aromatic H), 7.55-7.57 (m, 1H, aromatic H), 7.75-7.77 ppm (m, 2H, aromatic H). ^{13}C NMR (100 MHz, DMSO): δ = 41.47 (C4), 60.45 (C5), 112.57, 118.82, 125.75, 127.16, 127.89, 128.63, 128.83, 129.06, 129.27, 129.96, 131.08, 132.01, 138.78, 143.82, 147.48 ppm (aromatic C). UV ($CHCl_3$): λmax (log ε) = 355 nm (4.25), 316 (sh, 3.92), 240 (4.19).

*3-(4-Methoxyphenyl)-1,5-diphenyl-2-pyrazoline (**1h**)*

M.P. 141-143 ºC. IR (KBr): ν = 3086, 3026, 1600, 1560, 1496, 1454, 1386, 1321, 1255, 1114, 1019, 828, 746 cm^{-1}. ^{1}H NMR (400 MHz, DMSO-*d6*): δ = AMX- system, δ_A = 3.08 (J_{AM} = 17.4 Hz, J_{AX} = 6.6 Hz, 1H, 4-CH), 3.79 (s, 3H, OCH_3), δ_M = 3.90 (J_{AM} = 17.4 Hz, J_{MX} = 12.2 Hz, 1H, 4-CH), δ_x = 5.42 (J_{MX} = 12.2 Hz, J_{AX} = 6.6 Hz, 1H, 5-CH), 6.67-6.81 (m, 1H,

aromatic H), 6.97-7.01 (m, 4H, aromatic H), 7.12-7.16 (m, 2H, aromatic H), 7.24-7.36 (m, 5H, aromatic H), 7.68-7.71 ppm (m, 2H, aromatic H). ^{13}C NMR (100 MHz, DMSO-*d6*): δ = 43.24 (C4), 55.22, 63.07 (C5), 112.76, 114.11, 118.23, 124.86, 125.83, 127.25, 127.32, 128.79, 128.94, 142.69, l44.55, 147.22, 159.81 ppm (aromatic C). UV ($CHCl_3$): λ_{max} (log ε) = 354 nm (4.17), 321 (sh, 3.97), 250 (4.16).

*3-(3-Methoxyphenyl)-1,5-diphenyl-2-pyrazoline (**1i**)*

M.P. 126-128 ºC. IR (KBr): ν = 3028, 2966, 1588, 1557, 1496, 1460, 1380, 1265, 1213, 1127, 1030, 866, 744, 690 cm^{-1}. ^{1}H NMR (400 MHz, DMSO-*d6*): δ = AMX- system, δ_A = 3.11 (J_{AM} = 17.6 Hz, J_{AX} = 6.4 Hz, 1H, 4-CH), 3.81 (s, 3H, OCH_3), δ_M = 3.91 (J_{AM} = 17.6 Hz, J_{MX} = 12.4 Hz, 1H, 4-CH), δ_x = 5.48 (J_{MX} = 12.4 Hz, J_{AX} = 6.4 Hz, 1H, 5-CH), 6.70-6.74 (m, 1H, aromatic H), 6.93-6.96 (m, 1H, aromatic H), 7.01-7.03 (m, 2H, aromatic H), 7.14-7.18 (m, 2H, aromatic H), 7.24-7.36 ppm (m, 8H, aromatic H). ^{13}C NMR (100 MHz, DMSO-*d6*): δ = 46.34 (C4), 55.58, 63.08 (C5), 112.26, 112.85, 118.39, 120.64, 121.14, 125.77, 127.29, 128.09, 128.81, 128.95, 130.25, 142.73, 144.38, 146.41, 157.20 ppm (aromatic C). UV ($CHCl_3$): λ_{max} (log ε) = 360 nm (4.27), 241 (4.12).

*3-(2-Methoxyphenyl)-1,5-diphenyl-2-pyrazoline (**1j**)*

M.P. 160-163ºC. IR (KBr): ν = 3057, 2956, 1594, 1553, 1494, 1458, 1376, 1311, 1245, 1119, 1027, 867, 762 cm^{-1}. ^{1}H NMR (400 MHz, DMSO-*d6*): δ = AMX- system, δ_A = 3.17 (J_{AM} = 18.0 Hz, J_{AX} = 6.4 Hz, 1H, 4-CH), 3.77 (s, 3H, OCH_3), δ_M = 3.98 (J_{AM} = 18.0 Hz, J_{MX} = 12.0 Hz, 1H, 4-CH), δ_x = 5.39 (J_{MX} = 12.0 Hz, J_{AX} = 6.4 Hz, 1H, 5-CH), 6.68-6.72 (m, 1H, aromatic H), 6.98-7.08 (m, 4H, aromatic H), 7.12-7.16 (m, 2H, aromatic H), 7.23-7.38 (m, 6H, aromatic H), 7.90-7.93 ppm (m, 1H, aromatic H). ^{13}C NMR (100 MHz, DMSO-*d6*): δ = 46.34 (C4), 55.58, 63.08 (C5), 112.26, 112.85, 118.39, 120.64, 121.14, 125.77, 127.29, 128.09, 128.81, 128.95, 130.25, 142.73, 144.38, 146.41, 157.20 ppm (aromatic C). UV ($CHCl_3$): λmax (log ε) = 357 nm (4.34), 251 (4.28).

*5-(4-Methoxyphenyl)-1,3-diphenyl-2-pyrazoline (**1k**)*

M.P. 123-125 ºC. IR (KBr): ν = 3064, 2958, 1596, 1555, 1497, 1445, 1389, 1322, 1247, 1116, 1030, 873, 753 cm^{-1}. ^{1}H NMR (400 MHz, DMSO-*d6*): δ = AMX-system, δ_A = 3.08 (J_{AM} = 17.6 Hz, J_{AX} = 6.4 Hz, 1H, 4-CH), 3.71 (s, 3H, OCH_3), δ_M = 3.88 (J_{AM} = 17.6 Hz, J_{MX} = 12 Hz, 1H, 4-CH), δ_x = 5.43 (J_{MX} = 12 Hz, J_{AX} = 5.8 Hz, 1H, 5-CH), 6.69-6.73 (m, 1H, aromatic H), 6.88-6.91 (m, 2H, aromatic H), 7.00-7.03 (m, 2H, aromatic H), 7.13-7.17 (m, 2H, aromatic H), 7.20-7.22 (m, 2H, aromatic H), 7.35-7.39 (m, 1H, aromatic H), 7.41-7.45 (m, 2H, aromatic H), 7.74-7.76 ppm (m, 2H, aromatic H). ^{13}C NMR (100 MHz, DMSO-*d6*): δ = 42.94 (C4), 54.98, 62.60 (C5), 112.96, 114.29, 118.51, 125.62, 127.06, 128.63, 128.80, 132.31, 134.38, 144.20, 147.11, 158.43 ppm (aromatic C). UV ($CHCl_3$): λmax (log ε) = 357 nm (4.29), 315 (sh, 3.95), 239 (4.27).

*5-(3-Methoxyphenyl)-1,3-diphenyl-2-pyrazoline (**1l**)*

M.P. 92-95 ºC. IR (KBr): ν = 3085, 3056, 1595, 1557, 1494, 1451, 1390, 1327, 1262, 1128, 1049, 868, 752 cm^{-1}. ^{1}H NMR (400 MHz, DMSO-*d6*): δ = AMX-system, δ_A = 3.11 (J_{AM} = 17.4 Hz, J_{AX} = 6.4 Hz, 1H, 4-CH), 3.71 (s, 3H, OCH_3), δ_M = 3.91 (J_{AM} = 17.4 Hz, J_{MX} = 12.2 Hz, 1H, 4-CH), δ_x = 5.44 (J_{MX} = 12.2 Hz, J_{AX} = 6.4 Hz, 1H, 5-CH), 6.71-6.75 (m, 1H, aromatic H), 6.82-6.86 (m, 3H, aromatic H), 7.01-7.03 (m, 2H, aromatic H), 7.15-7.19 (m, 2H, aromatic H), 7.24-7.28 (m, 1H, aromatic H), 7.35-7.45 (m, 3H, aromatic H), 7.74-7.76 (m, 2H, aromatic H). ^{13}C NMR (400 MHz, DMSO-*d6*): δ = 42.88 (C4), 54.95, 63.09 (C5), 111.70, 112.42, 112.91, 117.77, 118.62, 125.66, 128.63, 128.69, 128.85, 130.20, 132.22, 144.16, 144.27, 147.26, 159.60 ppm (aromatic C). UV ($CHCl_3$): λ_{max} (log ε) = 356 nm (4.22), 241 (4.17).

*5-(2-Methoxyphenyl)-1,3-diphenyl-2-pyrazoline (**1m**)*

M.P. 130-132 ºC. IR (KBr): ν = 3029, 3004, 1592, 1566, 1492, 1458, 1389, 1322, 1235, 1130, 1024, 871, 747 cm^{-1}. ^{1}H NMR (400 MHz, DMSO-*d6*): δ = AMX-system, δ_A = 3.01 (J_{AM} = 17.4 Hz, J_{AX} = 6 Hz, 1H, 4-CH), 3.92 (s, 3H, OCH_3), δ_M = 3.92 (J_{AM} = 17.4 Hz, J_{MX} = 12.1 Hz, 1H, 4-CH), δ_x = 5.62 (J_{MX} = 12.1 Hz, J_{AX} = 6 Hz, 1H, 5-CH), 6.70-6.73 (m, 1H, aromatic H), 6.81-6.85 (m, 1H, aromatic H), 6.93-6.95 (m, 3H, aromatic H), 7.09-7.11 (m, 3H, aromatic H), 7.23-7.27 (m, 1H, aromatic H), 7.34-7.43 (m, 3H, aromatic H), 7.73-7.75 (m, 2H, aromatic H). ^{13}C NMR (100 MHz, DMSO-*d6*): δ = 41.64 (C4), 55.65, 57.52 (C5), 111.43, 112.50, 118.38, 120.60, 125.61, 125.90, 128.59, 128.63, 128.92, 129.15, 132.34, 144.04, 147.56, 155.95 ppm (aromatic C). UV ($CHCl_3$): λ_{max} (log ε) = 360 nm (4.27), 315 (sh, 3.92), 243 (4.24).

*3-(4-Nitrophenyl)-1,5-diphenyl-2-pyrazoline (**1n**)*

M.P. 180-183 ºC. IR (KBr): ν = 3064, 2931, 1593, 1546, 1499, 1455, 1390, 1337, 1244, 1140, 1105, 847, 745 cm^{-1}. ^{1}H NMR (400 MHz, DMSO-*d6*): δ = AMX-system, δ_A = 3.19 (J_{AM} = 17.6 Hz, J_{AX} = 6.2Hz, 1H, 4-CH), δ_M = 3.98 (J_{AM} = 17.6 Hz, J_{MX} = 12.6 Hz, 1H, 4-CH), δ_x = 5.65 (J_{MX} = 12.6 Hz, J_{AX} = 6.2 Hz, 1H, 5-CH), 6.77-6.81 (m, 1H, aromatic H), 7.07-7.09 (m, 2H, aromatic H), 7.17-7.22 (m, 2H, aromatic H), 7.25-7.30 (m, 3H, aromatic H), 7.34-7.37 ppm (m, 2H, aromatic H), 7.96 (d, J = 8.9 Hz, 2H, aromatic H), 8.26 ppm (d, J = 8.9 Hz, 2H, aromatic H). ^{13}C NMR (100 MHz, DMSO-*d6*): δ = 42.26 (C4), 63.56 (C5), 113.42, 119.65, 123.95, 125.80, 126.26, 127.58, 128.98, 129.06, 138.65, 141.97, 143.14, 145.04, 146.48 ppm (aromatic C). UV ($CHCl_3$): λmax (log ε) = 446 nm (4.35), 267 (4.21).

*3-(3-Nitrophenyl)-1,5-diphenyl--2-pyrazoline (**1o**)*

M.P. 134-136 ºC. IR (KBr): ν = 3029, 2902, 1594, 1527, 1495, 1455, 1389, 1319, 1248, 1121, 1071, 866, 743 cm^{-1}. ^{1}H NMR (400 MHz, DMSO-*d6*): δ = AMX-system, δ_A = 3.28 (J_{AM} = 17.6 Hz, J_{AX} = 6.3 Hz, 1H, 4-CH), δ_M = 4.05 (J_{AM} = 17.6 Hz, J_{MX} = 12.5 Hz, 1H, 4-

CH), δ_x = 5.66 (J_{MX} = 12.5 Hz, J_{AX} = 6.3 Hz, 1H, 5-CH), 6.81-6.85 (m, 1H, aromatic H), 7.11-7.13 (m, 2H, aromatic H), 7.23-7.27 (m, 2H, aromatic H), 7.31-7.44 (m, 5H, aromatic H), 7.76-7.80 (m, 1H, aromatic H), 8.18-8.20 (m, 1H, aromatic H), 8.24-8.27 (m, 1H, aromatic H), 8.55-8.56 ppm (m, 1H, aromatic H). ^{13}C NMR (100 MHz, DMSO-*d6*): δ = 42.50 (C4), 63.41 (C5), 113.17, 119.20, 119.53, 122.70, 125.83, 127.50, 128.93, 129.01, 130.25, 131.64, 133.95, 142.09, 143.55, 145.20, 148.11 ppm (aromatic C). UV ($CHCl_3$): λ_{max} (log ε) = 367 nm (4.35), 241 (4.32).

*3-(2-Nitrophenyl)-1,5-diphenyl--2-pyrazoline (**1p**)*

M.P. 146-148 ºC. IR (KBr): ν = 3028, 2904, 1594, 1536, 1496, 1455, 1389, 1323, 1248, 1137, 1069, 876, 748 cm^{-1}. ^{1}H NMR (400 MHz, DMSO-*d6*): δ = AMX-system, δ_A = 3.17 (J_{AM} = 17.4 Hz, J_{AX} = 6.4Hz, 1H, 4-CH), δ_M = 4.01 (J_{AM} = 17.4 Hz, J_{MX} = 12.4 Hz, 1H, 4-CH), δ_x = 5.59 (J_{MX} = 12.4 Hz, J_{AX} = 6.4 Hz, 1H, 5-CH), 6.77-6.81 (m, 1H, aromatic H), 6.92-6.94 (d, J = 8.0 Hz, 2H, aromatic H), 7.17-7.21 (m, 2H, aromatic H), 7.29-7.42 (m, 5H, aromatic H), 7.59-7.63 ppm (m, 1H, aromatic H), 7.71-7.72 (d, J = 4.0. Hz, 2H, aromatic H), 7.85-7.87 ppm (d, 7.9 Hz, 1H, aromatic H). ^{13}C NMR (100 MHz, DMSO-d6): δ = 43.27 (C4), 63.05 (C5), 112.97, 119.42, 123.28, 124.15, 125.86, 127.57, 128.91, 129.01, 129.09, 129.24, 131.65, 141.92, 142.16, 143.47, 148.06 ppm (aromatic C). UV ($CHCl_3$): λ_{max} (log ε) = 350 nm (4.13), 296 (sh, 3.96), 246 (4.27).

*5-(4-Nitrophenyl)-1,3-diphenyl-2-pyrazoline (**1q**)*

M.P. 113-116 ºC. IR (KBr): ν = 3057, 2910, 1592, 1567, 1496, 1447, 1382, 1318, 1242, 1104, 1067, 849, 750 cm^{-1}. ^{1}H NMR (400 MHz, DMSO-*d6*): δ = ABX-system, δ_A = 3.17 (J_{AB} = 17.6 Hz, J_{AX} = 6.3 Hz, 1H, 4-CH), δ_B = 3.98 (J_{AB} = 17.6 Hz, J_{BX} = 12.4 Hz, 1H, 4-CH), δ_x = 5.68 (J_{BX} = 12.4 Hz, J_{AX} = 6.3 Hz, 1H, 5-CH), 6.73-6.77 (m, 1H, aromatic H), 6.99-7.02 (m, 2H, aromatic H), 7.16-7.20 (m, 2H, aromatic H), 7.36-7.46 (m, 3H, aromatic H), 7.56-

7.58 (m, 2H, aromatic H), 7.75-7.77 (m, 2H, aromatic H), 8.20-8.23 ppm (m, 2H, aromatic H). ^{13}C NMR (100 MHz, DMSO-*d6*): δ = 42.54 (C4), 62.41 (C5), 112.94, 118.97, 124.26, 125.78, 127.32, 128.64, 128.89, 129.01, 131.94, 143.90, 146.82, 147.43, 150.01 ppm (aromatic C). UV ($CHCl_3$): λ_{max} (log ε) = 350 nm (4.31), 249 (4.32).

*5-(3-Nitrophenyl)-1,3-diphenyl-2-pyrazoline (**1r**)*

M.P. 123-125 ºC. IR (KBr): ν = 3030, 2923, 1593, 1565, 1498, 1446, 1386, 1354, 1241, 1116, 1064, 871, 700 cm^{-1}. ^{1}H NMR (400 MHz, DMSO-*d6*): δ = AMX-system, δ_A = 3.22 (J_{AM} = 17.4 Hz, J_{AX} = 6.2 Hz, 1H, 4-CH), δ_M = 3.98 (J_{AM} = 17.4 Hz, J_{MX} = 12.2 Hz, 1H, 4-CH), δ_x = 5.73 (J_{MX} = 12.2 Hz, J_{AX} = 6.2 Hz, 1H, 5-CH), 6.73-6.77 (m, 1H, aromatic H), 7.02-7.04 (m, 2H, aromatic H), 7.16-7.20 (m, 2H, aromatic H), 7.37-7.46 (m, 3H, aromatic H), 7.63-7.67 (m, 1H, aromatic H), 7.72-7.77 (m, 3H, aromatic H), 8.13-8.19 ppm (m, 2H, aromatic H). ^{13}C NMR (100 MHz, DMSO-*d6*): δ = 42.61 (C4), 62.19 (C5), 112.95, 118.99, 120.85, 122.49, 125.82, 128.66, 128.91, 129.04, 130.70, 131.95, 132.64, 143.90, 144.64, 147.56, 148.12 ppm (aromatic C). UV ($CHCl_3$): λmax (log ε) = 351 nm (4.20), 247 (4.26).

*5-(2-Nitrophenyl)-1,3-diphenyl-2-pyrazoline (**1s**)*

M.P. 136-138 ºC. IR (KBr): ν = 2846, 1596, 1523, 1497, 1444, 1392, 1337, 1264, 1128, 1066, 746, 689 cm^{-1}. ^{1}H NMR (400 MHz, DMSO-*d6*): δ = AMX-system, δ_A = 3.31 (J_{AM} = 17.8 Hz, J_{AX} = 5.8 Hz, 1H, 4-CH), δ_M = 4.08 (J_{AM} = 17.8 Hz, J_{MX} = 12.4 Hz, 1H, 4-CH), δ_x = 5.91 (J_{MX} = 12.4 Hz, J_{AX} = 5.6 Hz, 1H, 5-CH), 6.73-6.76 (m, 1H, aromatic H), 6.95-6.97 (m, 2H, aromatic H), 7.15-7.19 (m, 2H, aromatic H), 7.26-7.28 (m, 1H, aromatic H), 7.36-7.45 (m, 3H, aromatic H), 7.54-7.58 (m, 1H, aromatic H), 7.63-7.67 ppm (m, 1H, aromatic H), 7.75-7.77 (m, 2H, aromatic H), 8.15-8.17 (m, 1H, aromatic H). ^{13}C NMR (100 MHz, DMSO-*d6*): δ = 42.44 (C4), 59.81 (C5), 112.58, 118.86, 125.44, 125.77, 127.56, 128.62, 128.88,

128.96, 129.05, 131.96, 134.43, 136.38, 143.51, 147.32, 147.60 ppm (aromatic C). UV ($CHCl_3$): λ_{max} (log ε) = 353 nm (4.36), 313 (sh, 4.09), 243 (4.36).

Acknowledgement

We are thankful to the Research Council and Office of Graduate Studies of the University of Isfahan for their financial support.

Authors Information

*Phone: ++98 31 37934915, Fax: ++98 31 36689732. E-mail: memarian@sci.ui.ac.ir

*Phone: ++98 31 37934916, Fax: ++98 31 36689732. E-mail: sabzyan@sci.ui.ac.ir

Notes

E-mail: soltanimarzie@sci.ui.ac.ir

References

[1] D. Havrylyuk, B. Zimenkovsky, O. Vasylenko, A. Gzella, R. Lesyk, Synthesis of new 4-thiazolidinone, pyrazoline and isatin based conjugates with promising antitumor activity, J. Med. Chem. 55 (2012) 8630-8641. DOI: 10.1021/jm300789g

[2] Y.R. Prasad, A.L. Rao, L. Prasoona, K. Murali, P.R. Kumar, Synthesis and antidepressant activity of some 1,3,5-triphenyl-2-pyrazolines and 3-(2"-hydroxy naphthalen-1"-yl)-1,5-diphenyl-2-pyrazolines, Bioorg. Med. Chem. Lett. 15 (2005) 5030-5034. DOI: 10.1016/j.bmcl.20052007) 373-379. DOI: 10.1016/j.ejmech.2006.09.006.08.040

[3] Z. Ozdemir, H.B. Kandilici, B. Gumusel, U. Calis, A.A. Bilgin, Synthesis and studies on antidepressant and anticonvulsant activities of some 3-(2-furyl)-pyrazoline derivatives, Eur. J. Med. Chem. 42 (2007) 373-379. DOI: 10.1016/j.ejmech.2006.09.006

[4] S. Venkataraman, S. Jain, K. Shah, N. Upmanyu, Synthesis and biological activity of some novel pyrazolines, Acta. Pol. Pharm. 67 (2010) 361-366. DOI: (PMID: 20635531)

[5] A. Kumar, B.G. Varadaraj, R.K. Singla, Synthesis and evaluation of antioxidant activity of novel 3,5-disubstituted-2-pyrazolines, Bull. Fac. Pharm. (Cairo Univ) 67 (2013) 167-173. DOI: 10.1016/j.bfopcu.2013.04.002

[6] M. Amir, H. Kumar, S.A. Khan, Synthesis and pharmacological evaluation of pyrazoline derivatives as new anti-inflammatory and analgesic agents, Bioorg. Med. Chem. Lett. 18 (2008) 918-922. DOI: 10.1016/j.bmcl.2007.12.043

[7] B. Insuasty, A. Tigreros, F. Orozco, J. Quiroga, R. Abonia, M. Nogueras, A. Sanchez, J. Cobo, Synthesis of novel pyrazolic analogues of chalcones and their 3-aryl-4-(3-aryl-4,5-dihydro-1H-pyrazol-5-yl)-1-phenyl-1H-pyrazole derivatives as potential antitumor agents, Bioorg. Med. Chem. Lett. 18 (2010) 4965-4974. DOI: 10.1016/j.bmc.2010.06.013

[8] S.A.F. Rostom, M.H. Badr, H.A. Abd El Razik, H.M.A. Ashour, A.E. Abdel Wahab, Synthesis of some pyrazolines and pyrimidines derived from polymethoxy chalcones as anticancer and antimicrobial agents, Arch. Pharm. Chem. Life Sci. 344 (2011) 572-587. DOI: 10.1002/ardp.201100077

[9] G. Thirunarayanan, K.G. Sekar, SiO_2-H_2SO_4 catalysed, microwave-assisted cyclization cumacetylation of 2-propenones under solvent-free condition: synthesis and spectral correlations of some 1-acetyl pyrazolines, J. Taibah. Univ. Sci. 8 (2014) 124-136. DOI: 10.1016/j.jtusci.2013.11.003

[10] S.P. Sakthinathan, G. Vanangamudi, G. Thirunarayanan, Synthesis, spectral studies and antimicrobial activities of some 2-naphthyl pyrazoline derivatives, Spectrochim. Acta A. Mol. Biomol. Spectrosc. 95 (2012) 693-700. DOI: 10.1016/j.saa.2012.04.082

[11] J. Cody, S. Mandal, L. Yang, C.J. Fahrni, Differential tuning of the electron transfer parameters in 1,3,5-triarylpyrazolines: a rational design approach for optimizing the contrast ratio of fluorescent probes, J. Am. Chem. Soc. 130 (2008) 13023-13032. DOI: 10.1021/ja803074y

[12] C.J. Fahrni, L. Yang, D.G. VanDerveer, Tuning the photoinduced electron-transfer thermodynamics in 1,3,5-triaryl-2-pyrazoline fluorophores: x-ray structures, photophysical characterization, computational analysis, and in vivo evaluation, J. Am. Chem. Soc. 125 (2003) 3799-3812. DOI: 10.1021/ja028266o

[13] M. Verma, A.F. Chaudhry, C.J. Fahrni, Predicting the photoinduced electron transfer thermodynamics in polyfluorinated 1,3,5-triarylpyrazolines based on multiple linear free energy relationships, Org. Biomol. Chem. 7 (2009) 1536-1546. DOI: 10.1039/B821042J

[14] H.R. Memarian, M. Abdoli-Senejani, Ultrasound-assisted photochemical oxidation of unsymmetrically substituted 1,4-dihydropyridines, Ultrasonics Sonochem. 15 (2008) 110-114. DOI: 10.1016/j.ultsonch.2006.06.008

[15] H.R. Memarian, N. Jafarpour, A. Farhadi, Free-radical oxidation of 2-oxo-1,2,3,4-tetrahydropyrimidines, Monatsh. Chem. 143 (2012) 277-281. DOI: 10.1007/s00706-011-0573-8

[16] H.R. Memarian, E. Sanchooli, Substitution effects on the NMR and DFT studies of 4,6-diaryl-2-oxo-1,2,3,4-tetrahydropyrimidines, Magn. Reson. Chem. 54 (2016) 178-183. DOI: 10.1002/mrc.4360

[17] H.R. Memarian, H. Sabzyan, E. Sanchooli, DFT study of the molecular structure of 4,6-diaryl-2-oxo-1,2,3,4-tetrahydropyrimidines, Comp. Theo. Chem. 1093 (2016) 9-19. DOI: 10.1016/j.comptc.2016.07.019

[18] H.R. Memarian, M. Soleymani, H. Sabzyan, M. Bagherzadeh, H. Ahmadi, Voltammetric studies on 2-oxo-1,2,3,4-tetrahydropyrimidin-5-carboxamides: substituent effects, J. Phys. Chem. A, 115 (2011) 8264-8270. DOI: 10.1021/jp2014435

[19] H.R. Memarian, S. Ebrahimi, Light induced oxidation of 2,3-dihydroquinazolin-4(1*H*)-ones, J. Photochem. Photobiol. A: Chem. 271 (2013) 8-15. DOI: 10.1016/j.jphotochem.2013.07.008

[20] H.R. Memarian, S. Ebrahimi, Theoretical and voltammetric studies on the electron detachment process of 2,3-dihydroquinazolin-4(1*H*)-ones, Monatsh. Chem. 145 (2014) 1545-1554. DOI: 10.1007/s00706-014-1221-x

[21] H.R. Memarian, M. Kalantari, Steric and electronic substitution effects on the thermal oxidation of 5-carboethoxy-2-oxo-1,2,3,4-tetrahydropyridines, J. Iran. Chem. Soc. 14 (2017) 143-155. DOI: 10.1007/s13738-016-0966-z

[22] H.R. Memarian, M. Kalantari, H. Sabzyan, NMR and DFT Studies of 2-oxo-1,2,3,4-tetrahydropyridines; solvent and temperature effects, Aust. J. Chem. DOI: doi.org/10.1071/CH18018

[23] Z. Chen, C.S. Wannere, C. Corminboeuf, R. Puchta, P.V.R. Schleyer, Nucleus-independent chemical shifts (NICS) as an aromaticity criterion, Chem. Rev. 105 (2005) 3842-3888. DOI: 10.1021/cr030088+

[24] R. Gershoni-Poranne, Piecing it together: an additivity scheme for aromaticity using

NICS-XY-scans, Chem. Eur. J. 24 (2018) 4165-4172. DOI: 10.1002/chem.201705407

[25] M.P. Andersson, P. Uvdal, New scale factors for harmonic vibrational frequencies using the B3LYP density functional method with the triple-*ú* basis set 6-311+G(d,p), J. Phys. Chem. A 109 (2005) 2937-2941.

[26] Gaussian 09, Revision A.01, M.J. Frisch, G.W. Trucks, H.B. Schlegel, G.E. Scuseria, M.A. Robb, J.R. Cheeseman, G. Scalmani, V. Barone, B. Mennucci, G.A. Petersson, H. Nakatsuji, M. Caricato, X. Li,; H.P. Hratchian, A.F. Izmaylov, J. Bloino, G. Zheng, J.L. Sonnenberg, M. Hada, M. Ehara, K. Toyota, R. Fukuda, J. Hasegawa, M. Ishida, T. Nakajima, Y. Honda, O. Kitao, H. Nakai, T. Vreven, J.A. Montgomery, J.E. Peralta, F. Ogliaro, M. Bearpark, J.J. Heyd, E. Brothers, K.N. Kudin, V.N. Staroverov, R. Kobayashi, J. Normand, K. Raghavachari, A. Rendell, J.C. Burant, S.S. Iyengar, J. Tomasi, M. Cossi, N. Rega, J.M. Millam, M. Klene, J.E. Knox, J.B. Cross, V. Bakken, C. Adamo, J. Jaramillo, R. Gomperts, R.E. Stratmann, O. Yazyev, A.J. Austin, R. Cammi, C. Pomelli, J.W. Ochterski, R.L. Martin, K. Morokuma, V.G. Zakrzewski, G.A. Voth, P. Salvador, J.J. Dannenberg, S. Dapprich, A.D. Daniels, O. Farkas, J.B. Foresman, J.V. Ortiz, J. Cioslowski, D.J. Fox, Gaussian, Inc., Wallingford CT, 2009.

[27] M.J. Minch, Orientational dependence of vicinal proton-proton NMR coupling constants: the Karplus relationship, Concepts Magn. Reson. 6 (1994) 41-56. DOI: 10.1002/cmr.1820060104

[28] M. Homocianu, A. Airinei, D.O. Dorohoi, Solvent effects on the electronic absorption and fluorescence spectra, J. Adv. Res. Phys. 2 (2011) 1-9. DOI: 10.1.1.1007.2329&rep=rep1&type=pdf

[29] R.M. Silverstein, F.X. Webster, D. Kiemle, Spectrometric Identification of Organic Compounds; John Wiley & Sons, Inc., New York, 2005.

Research Highlights:

- Spectroscopic studies on the steric and electronic substituent effects in 2-pyrazolines.
- Study of experimental and theoretical NMR chemical shifts and coupling constants in 2-pyrazolines.
- σ- or π-donor/acceptor ability effects of the aryl substitutions on the spectral data.